Crystal and Molecular Structure of *cis*-[Pt(NH_3)$_2${d(pGpG)}], the Principal Adduct Formed by *cis*-Diamminedichloroplatinum(II) with DNA

Suzanne E. Sherman,[†] Dan Gibson,[†] Andrew H.-J. Wang,[‡] and Stephen J. Lippard*,[†]

Contribution from the Departments of Chemistry and Biology, Massachusetts Institute of Technology, Cambridge, Massachusetts 02139. *Received April 6, 1988*

Abstract: The crystal and molecular structures of *cis*-[Pt(NH_3)$_2${d(pGpG)}], the major adduct of the antitumor drug cisplatin covalently bound to its putative target on DNA, are reported. In the asymmetric unit, intermolecular hydrogen bonding and stacking interactions hold four crystallographically independent molecules together in a tightly packed aggregate, providing four examples of alternate conformations for this biologically important molecule. Tetrameric aggregates are separated from one another in the unit cell by solvent channels of varying diameters running parallel to the crystallographic axes. The conformations of the dinucleotides appear to be largely dependent on the requirements of platinum coordination. Thus, for each crystallographically independent molecule, platinum is coordinated in a square-planar mode to two cis ammine ligands and two guanine N7 atoms from the same dinucleotide, forcing the guanine bases to destack with resulting Gua/Gua dihedral angles ranging from 76.2 (5)° to 86.8 (6)°. Concomitant changes occur in torsion angles χ at the 5′- and 3′-ends of the dinucleotide, compared to the values typically found in DNA. The constraints of the dinucleotide backbone do, however, maintain the head-to-head orientation of the guanine bases. Overall, the backbone torsion angles at the 5′-end of each molecule resemble those in A-DNA. Backbone torsion angles at the 3′-ends are less easily categorized. In at least three of the four molecules, an intramolecular hydrogen bond occurs between a proton of an ammine ligand and an oxygen atom of the terminal 5′-phosphate, as had been previously predicted from molecular mechanics calculations. The molecule *cis*-[Pt(NH_3)$_2${d(pGpG)}] crystallizes in two forms, crystal type 1 having a = 31.326 (8) Å, b = 35.679 (9) Å, c = 19.504 (4) Å, Z = 16, space group $P2_12_12$ and crystal type 2 with a = 30.55 Å, b = 33.90 Å, c = 41.25 Å, Z = 32, space group $C222_1$. In the former crystal type, which forms the basis of the present discussion, 27 water and two glycine molecules as well as four platinated DNA fragments were located in the asymmetric unit.

There is considerable evidence that the widely used antitumor drug *cis*-diamminedichloroplatinum(II) (*cis*-DDP) exhibits its cytotoxicity by reacting with DNA.[1] Although similar quantities of bound *cis*-DDP and its stereoisomer, *trans*-DDP, inhibit SV40 DNA replication to the same extent in cell culture,[2] *trans*-DDP is clinically ineffective. In fact, much higher levels of *trans*-DDP than *cis*-DDP are required in cell media to produce equivalent bound drug-to-nucleotide ratios.[2,3] In order to gain an understanding of such behavior, it is of value to elucidate structural details of the different adducts formed by *cis*- and *trans*-DDP with DNA.

When *cis*-DDP reacts with DNA, there are several binding modes, including interstrand, intrastrand, and DNA-protein crosslinking.[1] Various mapping techniques[4,5a] have demonstrated that the main reaction product both in vitro and in vivo involves loss of two chloride ions and binding of platinum to the N7 atoms of adjacent guanine bases on the same strand. This d(GpG) intrastrand crosslink is uniquely formed by *cis*-DDP since the trans isomer does not link adjacent DNA bases but, rather, forms intrastrand adducts having one or more intervening nucleotides.[5]

Several attempts have been made to obtain detailed X-ray structural information about the reaction products of *cis*-DDP with DNA or RNA. When diffused into crystals of the double-stranded B-DNA dodecamer, [d(CpGpCpGpApApTpTpCpGpCpG)]$_2$, *cis*-DDP begins to bind monofunctionally to three guanosine N7 atoms.[6] Since no oligo(dG) sites are contained in this sequence, the main adduct produced by binding of platinum to DNA cannot form. Detailed geometric information concerning monofunctionally bound platinum was precluded owing to partial occupancy at three platinum sites. Other soaking experiments, with crystals of yeast phenylalanine transfer RNA ($tRNA^{Phe}$), have been carried out.[7] In one such experiment, monofunctional binding of platinum at two isolated guanosines of the biomolecule occurred.[7a] In a subsequent experiment, yeast $tRNA^{Phe}$ crystals were soaked in solutions containing hydrolysis products of *cis*-DDP.[7b] Electron density assigned to platinum was observed at d(GpG), d(ApG), and d(CpG) sequences, suggestive of bifunctional binding. In addition to partial occupancy of these platinum positions, however, the crystals were physically degraded, resulting in low resolution (~6 Å) data.

Attempts to model platinum–DNA interactions by allowing *cis*-DDP and its analogues to react with purine or pyrimidine bases, nucleosides, or nucleotides have generally yielded biologically improbable structures having C_2 molecular symmetry that imposes a head-to-tail orientation of bases.[8] Linkage of two purine bases via polymethylene chains has also failed to reproduce accurately the structure of platinum–DNA adducts, resulting instead in a dimeric structure.[9] A biologically relevant head-to-head platinum

[†] Department of Chemistry.
[‡] Department of Biology.

(1) (a) Sherman, S. E.; Lippard, S. J. *Chem. Rev.* **1987**, *87*, 1153. (b) Pinto, A. L.; Lippard, S. J. *Biochim. Biophys. Acta* **1985**, *780*, 167. (c) Roberts, J. J.; Pera, M. F., Jr. In *Platinum, Gold, and Other Metal Chemotherapeutic Agents*; Lippard, S. J., Ed.; ACS Symposium Series 209; American Chemical Society: Washington, DC, 1983.

(2) Ciccarelli, R. B.; Solomon, M. J.; Varshavsky, A.; Lippard, S. J. *Biochemistry* **1985**, *24*, 7533.

(3) Salles, B.; Butour, J.-L.; Lesca, C.; Macquet, J.-P. *Biochem. Biophys. Res. Commun.* **1983**, *112*, 555.

(4) (a) Fichtinger-Schepman, A. M. J.; van der Veer, J. L.; den Hartog, J. H. J.; Lohman, P. H. M.; Reedijk, J. *Biochemistry* **1985**, *24*, 707. (b) Plooy, A. C. M.; Fichtinger-Schepman, A. M. J.; Schutte, H. H.; Van Dijk, M.; Lohman, P. H. M. *Carcinogenesis* **1985**, *6*, 561. (c) Tullius, T. D.; Lippard, S. J. *J. Am. Chem. Soc.* **1981**, *103*, 4620. (d) Royer-Pokora, B.; Gordon, L. K.; Haseltine, W. A. *Nucleic Acids Res.* **1981**, *9*, 4595.

(5) (a) Pinto, A. L.; Lippard, S. J. *Proc. Natl. Acad. Sci. U.S.A.* **1985**, *82*, 4616. (b) van der Veer, J. L.; Ligtvoet, G. J.; van den Elst, H.; Reedijk, J. *J. Am. Chem. Soc.* **1986**, *108*, 3860. (c) Gibson, D.; Lippard, S. J. *Inorg. Chem.* **1987**, *26*, 2275. (d) Lepre, C.; Strothkamp, K.; Lippard, S. J. *Biochemistry* **1987**, *26*, 5651.

(6) Wing, R. M.; Pjura, P.; Drew, H. R.; Dickerson, R. E. *Embo. J.* **1984**, *3*, 1201.

(7) (a) Rubin, J. R.; Sabat, M.; Sundralingam, M. *Nucleic Acids Res.* **1983**, *11*, 6571. (b) Dewan, J. C. *J. Am. Chem. Soc.* **1984**, *106*, 7239.

(8) (a) Gellert, R. W.; Bau, R. *J. Am. Chem. Soc.* **1975**, *97*, 7379. (b) Bau, R.; Gellert, R. W. *Biochimie* **1978**, *60*, 1040. (c) Cramer, R. E.; Dahlstrom, P. L.; Seu, M. J. T.; Norton, T.; Kashiwagi, M. *Inorg. Chem.* **1980**, *19*, 148. (d) Marzilli, L. G.; Chalilpoyil, P.; Chiang, C. C.; Kistenmacher, T. J. *J. Am. Chem. Soc.* **1980**, *102*, 2480. (e) Kistenmacher, T. J.; Orbell, J. D.; Marzilli, L. G. In *Platinum, Gold, and Other Metal Chemotherapeutic Agents*; Lippard, S. J., Ed.; ACS Symposium Series 209; American Chemical Society: Washington, DC, 1983. (f) Orbell, J. D.; Marzilli, L. G.; Kistenmacher, T. J. *J. Am. Chem. Soc.* **1981**, *103*, 5126.

(9) Heyl, B. L.; Shinozuka, K.; Miller, S. K.; van der Veer, D. G.; Marzilli, L. G. *Inorg. Chem.* **1985**, *24*, 661.

0002-7863/88/1510-7368$01.50/0

complex was successfully synthesized by using the ligand 9-ethylguanine.[10] Although important details regarding the orientations of the guanine bases can be gained from this structure, it necessarily lacks information about the effects of platinum binding on the sugar-phosphate backbone.

Until recently, the best structural information about *cis*-DDP binding to DNA came from solution NMR studies of the *cis*-\{Pt(NH$_3$)$_2$\}$^{2+}$ fragment bound to short oligodeoxynucleotides.[11-16] These investigations have supplied many details about the time-averaged conformation of the *cis*-[Pt(NH$_3$)$_2$\{d(GpG)\}] adduct in solution. In order to gain more detailed structural information and, especially, metrical parameters, X-ray crystallographic information is required. The present article describes the X-ray structural characterization to atomic resolution of *cis*-[Pt(NH$_3$)$_2$\{d(pGpG)\}], the first such results of an antitumor drug covalently bound to its putative target on DNA. A preliminary report of part of this work has appeared.[17]

Experimental Section

Synthesis and Crystallization of *cis*-[Pt(NH$_3$)$_2$\{d(pGpG)\}]. The methods used to synthesize, purify, characterize, and crystallize *cis*-[Pt(NH$_3$)$_2$\{d(pGpG)\}] have been described previously.[17] Poorly formed, colorless prisms with approximate dimensions of 0.8 mm × 0.25 mm × 0.1 mm (crystal type 2) appeared after 2 weeks from solutions containing 33 mM glycine·HCl (pH 3.8) or sodium acetate (pH 3.9) buffer, 33 mM NaCl, 9.2% 2-methyl-2,4-pentanediol (2-MPD), and 9 mM platinum complex, equilibrated to 70% 2-MPD at room temperature. Colorless, regularly formed rectangular parallelepipeds with approximate dimensions of 0.6 mm × 0.5 mm × 0.4 mm (crystal type 1) appeared after $7^1/_2$ months from similar glycine·HCl solutions to which had been added 17 mM $MgCl_2$. Both crystal forms were mounted and sealed in glass capillaries containing a drop of mother liquor for study on the diffractometer.

Collection and Reduction of X-ray Data. Axial photographs and unit cell parameters revealed that both crystal forms belong to the orthorhombic system. Three data sets were collected on three different crystals of type 2; for one crystal, monochromated Mo Kα radiation on an Enraf-Nonius CAD-4F diffractometer at 25 °C was used, and for two crysals, Cu Kα radiation on Nicolet P3 diffractometers was employed at 16 °C and −12 °C, respectively. The highest resolution data (1.37 Å; 4677 reflections) were collected on the crystal for which Mo Kα radiation was used. Unit cell dimensions of all three crystals were similar. A significant amount of radiation decay was observed during data collection on type 2 crystals. Data for crystal type 1 were collected on a Nicolet P3 diffractometer by using Cu Kα radiation and the ω scan mode at 16 °C. Because of the large amount of decay observed in crystals of type 2, data collection was carried out at a scan rate of 4°/min for $0 \le \theta \le 45°$ (1.09 Å resoltuion) and 3°/min for $45° \le \theta \le 55°$ (0.94 Å resolution). From the systematic absences, the space group for crystal type 1 was found to be $P2_12_12$.[18] The space group for crystal type 2 was determined to be either $C222$ or $C222_1$, since the systematic absence of 00 l reflections, where l = odd, was ambiguous. The choice of space group for crystal type 2 was decided by successful refinement. Unit cell parameters for both crystal forms and data collection procedures for crystal type 1 are contained in Table I. Further details about crystal type 2 will be reported subsequently.

Table I. Experimental Details of the X-ray Diffraction Study of *cis*-[Pt(NH$_3$)$_2$\{d(pGpG)\}]

crystal type 1[a]	crystal type 2[b]
(A) Crystal Parameters	
a = 31.326 (8) Å	a = 30.55 Å
b = 35.679 (9) Å	b = 33.90 Å
c = 19.504 (4) Å	c = 41.25 Å
cryst syst orthorhombic	cryst syst orthorhombic
space group $P2_12_12$	space group $C222_1$
Z = 16	Z = 32
V = 21 799 Å^3	V = 42 709 Å^3
(B) Measurement of Intensity Data (Crystal Type 1)	
instrument	Nicolet P3 diffractometer
radiation	Cu Kα (λ = 1.5418 Å)
no. of reflcns collected	14 950 [$2° < 2\theta < 110°$ ($+h,+k,+l$)]
no. of unique data	13 490, 10 255 of which have $F > 4\sigma(F)$
(C) Final Model from Unrestrained Least-Squares Refinement (Crystal Type 1)	
final R values[25]	R_1 = 0.082, R_2 = 0.091
no. of observatns[c]	10 235
no. of parameters	1121
resolution	0.94 Å
formula[d]	$Pt_1P_2O_{20.125}N_{12.5}C_{21}H_{44.75}$
formula wt	1051.44
ρ(calcd)	1.282 g/cm^3

[a] From least-squares refinement of the setting angles of 11 carefully centered reflections with $2\theta > 40°$. [b] Data from the original Mo data set of crystal type 2 are presented. [c] 10 255 − 20 reflections thought to be affected by secondary extinction. [d] Includes water and glycine molecules found in the crystal lattice.

Data collected on crystal type 1 were corrected for Lorentz polarization (LP) effects and were scaled for 22.4% (1.5% per 1000 reflections) decay. An empirical absorption correction was applied (μ = 56.6 cm^{-1}).[19] Averaging of equivalent reflections gave 13 490 unique data of which the 10 255 with $F_o > 4\sigma(F_o)$ were used in the structure solution and refinement.

Solution and Refinement of Structure for Crystal Type 1. Atomic coordinates of four crystallographically independent platinum atoms were determined by direct methods with MULTAN.[20] The remaining non-hydrogen atoms were located from a series of difference Fourier maps.[21] Unrestrained least-squares refinement was carried out in blocks with an enlarged version of SHELX-76.[22] Platinum, phosphorus, and phosphate oxygen atoms were refined anisotropically, and all other atoms were assigned isotropic thermal parameters. Neutral atom scattering factors and anomalous dispersion corrections were obtained from ref 23, and hydrogen atom scattering factors from ref 24. Refinement blocks consisted of pairs of platinum molecules. Each platinum molecule was also paired with the full set of located solvent and glycine molecules. Unit weights were used during every stage of the refinement.

(10) (a) Lippert, B.; Raudaschl, G.; Lock, C. J. L.; Pilon, P. *Inorg. Chim. Acta* **1984**, *93*, 43. (b) Schöllhorn, H.; Raudaschl-Sieber, G.; Müller, G.; Thewalt, U.; Lippert, B. *J. Am. Chem. Soc.* **1985**, *107*, 5932.

(11) Girault, J.-P.; Chottard, G.; Lallemand, J.-Y.; Chottard, J.-C. *Biochemistry* **1982**, *21*, 1352.

(12) den Hartog, J. H. J.; Altona, C.; Chottard, J.-C.; Girault, J.-P.; Lallemand, J.-Y.; de Leeuw, F. A. A. M.; Marcelis, A. T. M.; Reedijk, J. *Nucleic Acids Res.* **1982** *10*, 4715.

(13) (a) Marcelis, A. T. M.; den Hartog, J. H. J.; van der Marel, G. A.; Wille, G.; Reedijk, J. *Eur. J. Biochem.* **1983**, *135*, 343. (b) den Hartog, J. H. J.; Altona, C.; van der Marel, G. A.; Reedijk, J. *Eur. J. Biochem.* **1985**, *147*, 371.

(14) (a) Girault, J.-P.; Chottard, J.-C.; Guittet, E. R.; Lallemand, J.-Y.; Huynh-Dinh, T.; Igolen, J. *Biochem. Biophys. Res. Commun.* **1982**, *109*, 1157. (b) Neumann, J. M.; Tran-Dinh, S.; Girault, J.-P.; Chottard, J.-C.; Huynh-Dinh, T.; Igolen, J. *Eur. J. Biochem.* **1984**, *141*, 465. (c) van Hemelryck, B.; Guittet, E.; Chottard, G.; Girault, J.-P.; Huynh-Dinh, T.; Lallemand, J.-Y.; Igolen, J.; Chottard, J.-C. *J. Am. Chem. Soc.* **1984**, *106*, 3037. (d) van Hemelryck, B.; Guittet, E.; Chottard, G.; Girault, J.-P.; Herman, F.; Huynh-Dinh, T.; Lallemand, J.-Y.; Igolen, J.; Chottard, J.-C. *Biochem. Biophys. Res. Commun.* **1986**, *138*, 758.

(15) (a) Caradonna, J. P., Ph.D. Dissertation, Columbia University, 1985. (b) Caradonna, J. P.; Lippard, S. J. *Inorg. Chem.* **1988**, *27*, 1454.

(16) (a) den Hartog, J. H. J.; Altona, C.; van Boom, J. H.; van der Marel, G. A.; Haasnoot, C. A. G.; Reedijk, J. *J. Am. Chem. Soc.* **1984**, *106*, 1528. (b) den Hartog, J. H. J.; Altona, C.; van Boom, J. H.; van der Marel, G. A.; Haasnoot, C. A. G.; Reedijk, J. *J. Biomol. Struct. Dynamics* **1985**, *2*, 1137.

(17) Sherman, S. E.; Gibson, D.; Wang, A. H.-J.; Lippard, S. J. *Science (Washington, D.C.)* **1985**, *230*, 412.

(18) *International Tables for Crystallography*; Hahn, T., Ed.; D. Reidel Publishing Company: Dordrecht, Holland/Boston, MA, 1983; Vol. A, p 195.

(19) The empirical absorption correction was performed from ψ-scans of suitable reflections with χ close to 90°, as detailed in the following: North, A. C. T.; Phillips, D. C.; Mathews, F. S. *Acta Crystallogr.* **1968**, *A24*, 351.

(20) Main, P.; Lessinger, L.; Woolfson, M. M.; Germain, G.; Declercq, J.-P. MULTAN77, *A System of Computer Programs for the Automatic Solution of Crystal Structures from X-ray Diffraction Data*; University of York, York, England and University of Louvain, Louvain, Belgium, 1977.

(21) The positions of most atoms were found on difference Fourier maps generated by SHELX-76 (ref 22). The positions of the remaining atoms were found by stacking contoured Fourier map sections on plastic sheets. Phases for the latter Fourier maps were calculated by ORXFLS, and the maps were calculated and contoured with in-house programs.

(22) Sheldrick, G. M. In *Computing in Crystallography*; Schenk, H., Olthof-Hazenkamp, R., van Konigsveld, H., Bassi, G. C., Eds.; Delft University Press: Delft, The Netherlands, 1978. We thank G. M. Sheldrick for kindly providing a version of SHELX-76 extended by D. Rabinovich and K. Reich to handle 400 atoms and 500 variable parameters.

(23) *International Tables for X-ray Crystallography*; Kynoch Press: Birmingham, England, 1974; Vol. IV, pp 99, 149.

(24) Stewart, R. F.; Davidson, E. R.; Simpson, W. T. *J. Chem. Phys.* **1965**, *42*, 3175.

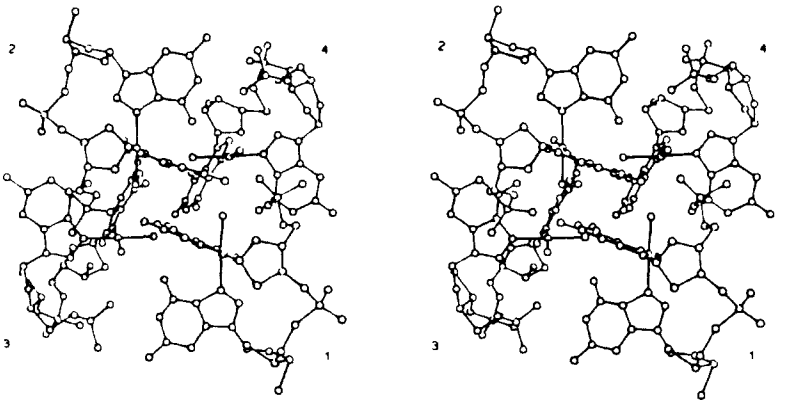

Figure 1. Stereoview of the four crystallographically independent *cis*-[$Pt(NH_3)_2${d(pGpG)}] molecules comprising the asymmetric unit. The view is down a pseudo-2-fold symmetry axis corresponding to the crystallographic [100] direction. The labels 1, 2, 3, and 4 refer to independent molecules 1–4. Solvent molecules in the lattice are not shown.

In the previously published model, refined to discrepancy indices of $R_1 = 0.0843$ and $R_2 = 0.0955$,[25] 26 water molecules and one glycine molecule were included in the refinement.[17] Eight strong water peaks at short distances (<2.4 (2) Å) to one another were assigned half-occupancy. Nineteen low angle reflections for which $F_o \leq 0.8F_c$, thought to be the result of secondary extinction effects, were omitted from the final least-squares cycles of the original model.

In subsequent refinements, the 19 low angle reflections which had been removed previously were reintroduced. The positions of the 5′- and 3′-guanine ring and 5′- and 3′-sugar hydrogen atoms were calculated based on C–H and N–H distances of 0.95 Å, and these hydrogen atoms were constrained to "ride" on the atoms to which they are attached. Amino hydrogen atoms attached to N2 of guanine were placed in the guanine plane. Positions of the remaining hydrogen atoms were neither located nor calculated. Separate overall temperature factors were refined for the sets of guanine hydrogen atoms, 5′-sugar hydrogen atoms and 3′-sugar hydrogen atoms. The thermal parameter for the 3′-sugar hydrogen atoms refined to the unacceptably large value of $U > 5.0$ Å^2, so these hydrogen atoms were removed. Three atoms originally thought to be disordered water molecules and assigned half-occupancy were subsequently assigned to a second molecule of glycine. Although this glycine molecule appeared on difference Fourier maps with reasonable geometry, attempts to refine the positions of its atoms resulted in poor geometry. Therefore, its geometry was constrained to that originally obtained from the maps, and only its thermal parameters were allowed to refine. Four new water molecules which exhibited reasonable hydrogen bonding geometry to atoms already located, and which refined to well-defined positions,[26] were included giving a total of 27 water molecules. At this stage, 20 strong low-angle reflections had $F_o \leq 0.8F_c$, probably as a result of secondary extinction effects, and they were omitted from the final refinement cycles. Four reflections omitted during refinement of the original model were not included in this set. Introduction of hydrogen atoms into the calculated model decreased the disparity between F_o and F_c for these four reflections.

Toward the end of the refinement, it became apparent from difference Fourier maps that the C4′ and C5′ atoms of the 3′-sugar residue of molecule 2 were disordered over two positions. Accordingly, this disorder was modelled in the refinement. Occupancy factors for the two conformations (**a** and **b**) of these atoms in molecule 2 refined to values of 0.46 (6) and 0.54 (6), respectively. Thermal parameters (U) for both C4′ atoms were constrained to 0.11 Å^2, and those for both C5′ atoms, to 0.18 Å^2. Positional parameters for both C4′ atoms oscillated about their mean positions during subsequent refinements. Therefore, they were fixed to these positions. Conformation **a** corresponds to that of molecule 2 observed in the original refinement.[17]

The refinement converged to the discrepancy indices reported in Table I. The overall thermal parameter (U) for hydrogen atoms bonded to guanine atoms refined to a value of 0.10 (6) Å^2. That for hydrogen atoms bonded to 5′-sugar atoms refined to a value of 0.08 (4) Å^2. The largest peak of residual electron density in the final difference Fourier map had a height of 0.91 e Å^{-3} and was <1.4 Å away from a platinum atom. Remaining electron density peaks in the map were either close to platinum atoms or in regions where disordered solvent molecules are expected to occur. The maximum value of the ratio of positional shift to estimated standard deviation was 0.248 for the y-coordinate of N1 in the 3′-guanosine of molecule 2. Observed and calculated structure factor amplitudes are available as Supplementary Material (Table S1).

Table II. Geometric Features of the Platinum Coordination Spheres of *cis*-[$Pt(NH_3)_2${d(pGpG)}]

(A) Bond Distances and Angles[a]

	molecule 1	molecule 2	molecule 3	molecule 4
Pt–N1	2.03 (2)	2.01 (2)	2.08 (2)	2.08 (2)
Pt–N2	2.03 (3)	2.09 (2)	2.04 (3)	2.06 (3)
Pt–N7A	2.01 (2)	2.02 (2)	1.91 (3)	1.93 (3)
Pt–N7B	2.05 (2)	1.95 (3)	2.00 (3)	2.06 (3)
N7A–Pt–N1	88.6 (9)	90.3 (9)	91 (1)	88.4 (9)
N7A–Pt–N2	179 (1)	173.3 (8)	178 (1)	177 (1)
N7A–Pt–N7B	89.1 (9)	90 (1)	85 (1)	89 (1)
N1–Pt–N2	92.0 (9)	90.8 (9)	91 (1)	93 (1)
N1–Pt–N7B	176.5 (9)	179 (1)	173 (1)	175 (1)
N2–Pt–N7B	90.3 (9)	89 (1)	93 (1)	89 (1)

(B) Dihedral Angles[b]

molecule	3′-Gua/5′-Gua	5′-Gua/PtN_4	3′-Gua/PtN_4
1	76.2 (5)	110.6 (5) [3.30 (3)]	86.1 (5)
2	81.0 (5)	110.8 (5) [3.49 (3)]	95.5 (5)
3	86.8 (6)	81.0 (6)	58.0 (6) [3.11 (4)]
4	80.6 (5)	76.6 (6)	59.6 (6) [3.18 (4)]

[a] Bond distances are in Å and angles are in deg. [b] Conventions used for assigning base/base and base/PtN_4 dihedral angles can be found in ref 8f and in Figure 3. The numbers in square brackets refer to the corresponding N(ammine)···O6 distance, in Å (see text).

Conformational Modelling. Studies of the conformations adopted by the crystallographically independent *cis*-[$Pt(NH_3)_2${d(pGpG)}] molecules were carried out on an Evans and Sutherland PS-300 terminal, with graphics programs FRODO[27] and HYDRA.[28] For these manipulations, the positions of ammonia hydrogen atoms were calculated at N–H distances of 1.01 Å, with SHELX-76.[22]

Results

Two morphologically distinct crystals of *cis*-[$Pt(NH_3)_2${d(pGpG)}] were grown under slightly different buffer conditions. Type 2 crystals were plate-like, nonuniform in appearance, and of overall poor quality. Type 1 crystals were of much better quality, diffracting to a Bragg angle of 110° in 2θ ($\lambda = 1.5418$ Å). Although interpretation of the Patterson map was complicated by the presence of 16 heavy atoms in the unit cell, satisfactory solution of the structure of crystal type 1 was afforded by direct methods.

Molecular Geometry of *cis*-[$Pt(NH_3)_2${d(pGpG)}]. Positional and thermal parameters from unrestrained refinement of crystal type 1 are reported in Tables S2 and S3 (Supplementary Mate-

(25) $R_1 = \sum||F_o| - |F_c||/\sum|F_o|$; $R_2 = [\sum w(|F_o| - |F_c|)^2/\sum w|F_o|^2]^{1/2}$.
(26) (a) Neidle, S.; Berman, H. M.; Shieh, H. S. *Nature (London)* **1980**, *288*, 129. (b) McCall, M.; Brown, T.; Kennard, O. *J. Mol. Biol.* **1985**, *183*, 385.
(27) Jones, T. A. "Frodo: A Graphics Fitting Program for Macromolecules", In *Computational Crystallography*; Sayre, D., Ed.; Clarendon Press: Oxford, England, 1982; p 303.
(28) HYDRA was written by Dr. R. Hubbard, Chemistry Department, University of York, York, England.

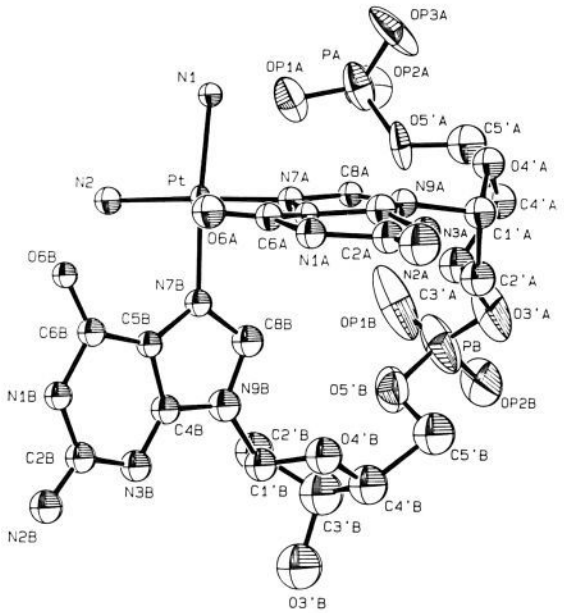

Figure 2. Molecular structure of molecule 4 in the asymmetric unit of *cis*-[Pt(NH$_3$)$_2$\{d(pGpG)\}] showing the atom labeling scheme. Labels C4A and C5A of the 5′-guanine base were omitted for clarity.

rial). Four *cis*-[Pt(NH$_3$)$_2$\{d(pGpG)\}] molecules, designated 1–4, comprise the asymmetric unit. In Figure 1, this tightly packed tetrameric aggregate is displayed as viewed down *a*. Noncrystallographic 2-fold symmetry along this axis relates pairs of molecules 1 and 2, designated class I, and molecules 3 and 4, designated class II.

Tables S4 and S5 contain complete bond distance and angle information about the four platinum and two glycine molecules contained in the asymmetric unit. A summary of salient features of the Pt coordination geometry appears in Table II. Unrestrained refinement resulted in a structure with some unusual bond distances and angles, especially for the 3′-sugars of the dinucleotide. Moreover, many atoms of the 3′-sugars and the phosphate groups have large thermal parameters, indicating either substantial thermal motion or unresolved disorder. Restrained refinement was carried out in an attempt to clarify the structure in the vicinity of the 3′-sugars.[29] Although this refinement led to improved bond lengths and angles, resulting in better agreement among the four independent molecules, it was not possible to define a specific disordered model from the residual electron density around the 3′-sugars. Some disorder in the 3′-sugar of molecule 2 was resolved, however, in unrestrained refinements. From the resulting geometries of the two disordered conformations, it seems likely that further disorder, which was not clearly observed in difference Fourier maps, also occurs. Specifically, an unusually long C3′B–C4′B bond of 2.13 Å and a relatively large C3′B–C4′B–C5′B angle of 138° occurs in conformation **a**. In conformation **b**, an unusually long C4′B–O4′B bond of 1.73 Å and a relatively large O4′B-C4′B-C3′B angle of 136° occurs. Different positions for C3′B in conformation **a** and for O4′B in conformation **b** could improve these geometries, but these positions could not be obtained from our data.

In all four molecules, platinum is coordinated in a square-planar mode to two cis ammine ligands and to two guanine N7 atoms of the dinucleotide, closing a 17-membered chelate ring (Figure 2). The mean Pt–NH$_3$ and Pt–N7 bond lengths, 2.05 and 1.99 Å, respectively, and adjacent N–Pt–N bond angles of ~90° reveal no steric constraints imposed by the chelating dinucleotide. The average guanine C5–N7–C8 angles from both unrestrained and restrained[29] refinements are a few degrees larger than the value of 104.2° observed for neutral guanine.[30] This increase is similar to that which occurs upon protonation of N7.[31]

The protonated oxygen atom of the 5′-phosphate group could not be differentiated from unprotonated oxygen atoms from the P–O distances and O–P–O interbond angles obtained in the unrestrained refinement.[31] For molecules 1 and 3, there seems to be one longer P–O bond, but for molecules 2 and 4, all P–O distances in the 5′-phosphate are equivalent.

Best planes through the guanine ring and platinum coordination planes, calculated by using coordinates from the unrestrained refinement, demonstrate that no atom deviates by more than 0.12 Å from the five atoms comprising the platinum coordination spheres of the four molecules (Table S6). No atom deviates by more than 0.17 Å from the 11 atoms contained in the guanine base planes. Platinum does not deviate by more than 0.4 Å from the guanine planes to which it is coordinated in any of the molecules.

The head-to-head arrangement of guanine bases, with both guanine O6 atoms situated on the same side of the PtN$_4$ plane, may be seen in Figure 2. Binding of two guanine N7 atoms to platinum in a cis geometry destacks the bases, resulting in base/base dihedral angles ranging from 76.2 (5)° to 86.8 (6)° (Table II). The guanine base planes are not strictly perpendicular to the platinum coordination plane but are tipped by 5°–32°, resulting in Gua/PtN$_4$ dihedral angles ranging from 58.0 (6)° to 110.8 (5)°. These angles are similar for pairs of molecules 1 and 2 and 3 and 4, reflecting the pseudo-2-fold symmetry of the crystal lattice (Figure 3).

In Table III are listed torsion angles for *cis*-[Pt(NH$_3$)$_2$\{d(pGpG)\}] and comparative values for crystals of A-DNA and B-DNA. Backbone, sugar, and glycosyl torsion angles for molecules 1, 3, and 4, and conformation **a** of molecule 2, fall near or within the ranges of values observed in crystallographic studies of A-type and B-type DNAs.[26b,32–39] For conformation **b** of molecule 2, α_B and γ_B lie outside these ranges. In some instances, variations in torsion angles among the four independent platinum molecules reflect differences between the two conformational classes (I and II) of molecules found in the crystal lattice.

The glycosyl torsion angle, χ, dictates the orientation of the base relative to the deoxyribose ring within a nucleotide. The χ_A and χ_B values of molecule 1 are near the "high-anti" range,[41] as is χ_A of molecule 2. χ_B of molecule 2 is somewhat more negative than that of molecule 1 and within the normal "anti" range. The glycosyl torsion angles of molecules 3 and 4 all fall within the "anti" range, with χ_A being 15°–20° more negative than χ_B.

The pseudorotation angles, P, and the amplitudes, ψ, which describe the sugar puckers of the 5′- and 3′-nucleotides have been calculated from the deoxyribose torsion angles, ν_0–ν_4 (see Table III).[40,42] The 5′-sugars of all four molecules have classical A-DNA puckers, either C2′-exo (class I molecules) or C3′-endo (class II molecules). The puckers of the 3′-sugars are somewhat more

(29) Sherman, S. E., Ph.D. Dissertation, Massachusetts Institute of Technology, 1987.

(30) Taylor, R.; Kennard, O. *J. Am. Chem. Soc.* **1982**, *104*, 3209.
(31) Taylor, R.; Kennard, O. *J. Mol. Struct.* **1982**, *78*, 1.
(32) Arnott, S.; Chandrasekaran, D. L.; Birdsall, A. G. W. L.; Ratcliff, R. L. *Nature (London)* **1980**, *283*, 743.
(33) (a) Dickerson, R. E.; Drew, H. R. *J. Mol. Biol.* **1981**, *149*, 761. (b) Fratini, A. V.; Kopka, M. L.; Drew, H. R.; Dickerson, R. E. *J. Biol. Chem.* **1982**, *257*, 14686.
(34) Wang, A. H.-J.; Fujii, S.; van Boom, J.; Rich, A. *Proc. Natl. Acad. Sci. U.S.A.* **1982**, *79*, 3968.
(35) Viswamitra, M. A.; Shakked, Z.; Jones, P. G.; Sheldrick, G. M.; Salisbury, S. A.; Kennard, O. *Biopolymers* **1982**, *21*, 513.
(36) Shakked, Z.; Rabinovich, D.; Kennard, O.; Cruse, W. B. T.; Salisbury, S. A.; Viswamitra, M. A. *J. Mol. Biol.* **1983**, *166*, 183.
(37) Conner, B. N.; Yoon, C.; Dickerson, J. L.; Dickerson, R. E. *J. Mol. Biol.* **1984**, *174*, 663.
(38) (a) Kennard, O. *J. Biomolec. Struct. Dyn.* **1985**, *3*, 205. (b) Cruse, W. B. T.; Salisbury, S. A.; Brown, T.; Cosstick, R.; Eckstein, F.; Kennard, O. *J. Mol. Biol.* **1986**, *192*, 891.
(39) Privé, G. G.; Heinemann, U.; Chandrasegaran, S.; Kan, L.-S.; Kopka, M. L.; Dickerson, R. E. *Science (Washington, D.C.)* **1987**, *238*, 498.
(40) IUPAC-IUB Joint Commission on Biochemical Nomenclature report, *Eur. J. Biochem.* **1983**, *131*, 9.
(41) Saenger, W. *Principles of Nucleic Acid Structure*; Springer-Verlag: New York, 1984.
(42) Altona, C.; Sundralingam, M. *J. Am. Chem. Soc.* **1972**, *94*, 8205.

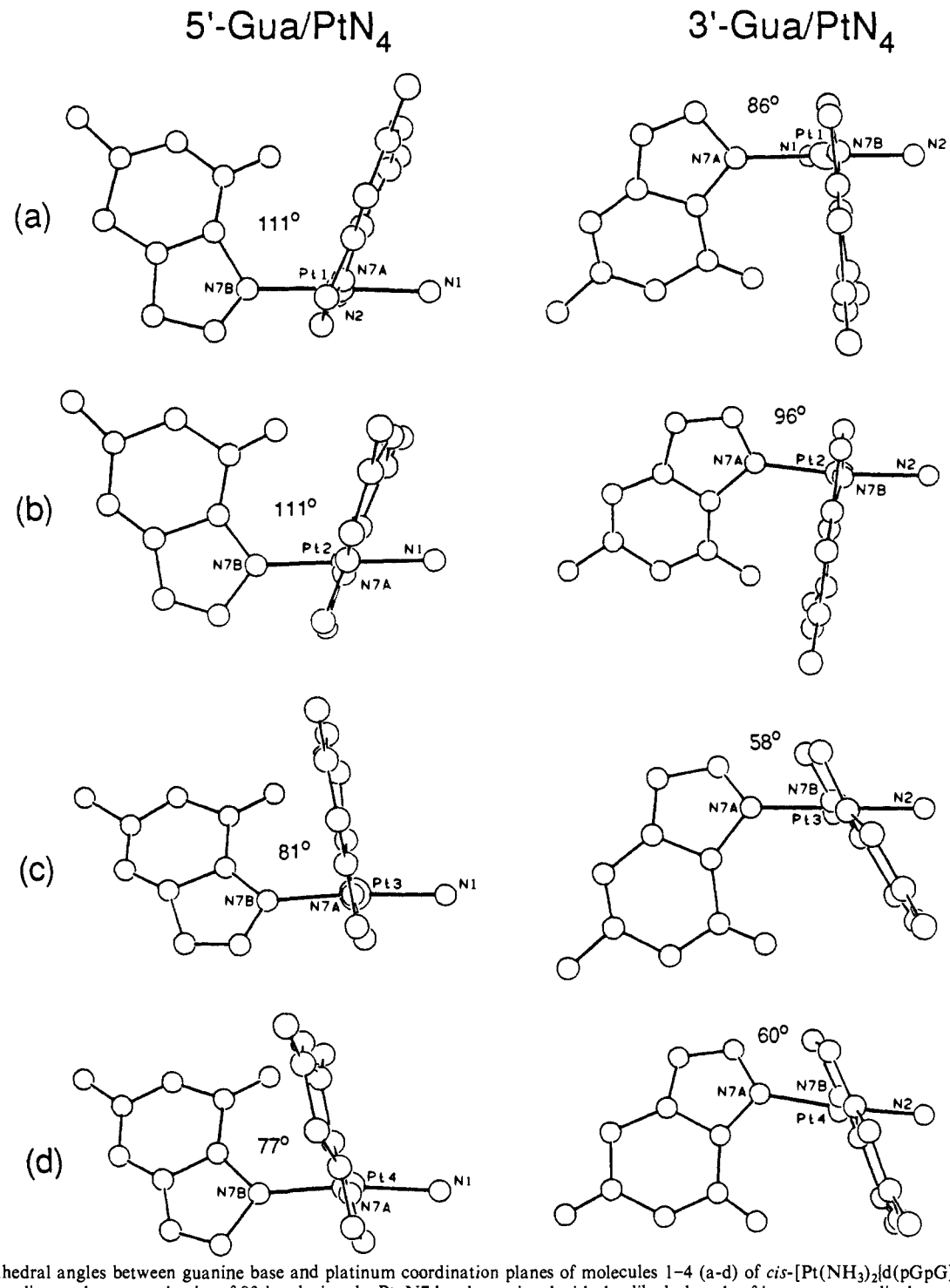

Figure 3. Dihedral angles between guanine base and platinum coordination planes of molecules 1–4 (a-d) of *cis*-[Pt(NH$_3$)$_2$[d(pGpG)]]. Angles are measured according to the convention in ref 8f, by placing the Pt–N7 bond associated with the dihedral angle of interest perpendicular to, and projecting out of, the plane of the paper. The opposite base is positioned to the left of the diagram, as shown. The sugar-phosphate backbones were omitted for clarity.

variable owing to conformational flexibility and/or disorder in the crystal lattice. All of the 3′-sugar conformations fall between O4′-endo and C2′-endo reference points on the pseudorotation cycle, characteristic of classical B-DNA structures.

Torsion angles δ are dictated by the different types of sugar pucker at the 5′- and 3′-ends of the molecules and have values of 91°–102° at the 5′-end and 140°–166° at the 3′-end. Torsion angles ϵ_A, ζ_A, α_B, and β_B specify the conformations of the phosphodiester linkages. Rotations about the C3′A–O3′A phosphodiester bond (ϵ_A) fall within the normal -ac range[43] seen in both A- and B-DNAs. Rotations about O3′A-PB (ζ_A), which fall within the -sc range,[43] are less negative than the average value seen in B-DNA. Instead, the values for ζ_A are closer to those observed in crystallographic studies of A-DNA.

Values for torsion angle α_B in molecules 1, 3, 4 and conformation **a** of molecule 2 all fall within the -sc (-gauche) range[43] and lie near or within the normal ranges observed in both A-DNA and B-DNA. In conformation **b** of molecule 2, α_B is trans, characteristic of nonhelicity.[41] Similar values have been observed crystallographically in yeast phenylalanine tRNA.[44]

(43) For definitions of the terms ±synperiplanar (±sp), ±synclinical (±sc), ±anticlinical (±ac), and ±antiperiplanar (±ap), see ref 40 or 41.

(44) Holbrook, S. R.; Sussman, J. L.; Warrant, R. W.; Kim, S.-H. *J. Mol. Biol.* **1978**, *123*, 631.

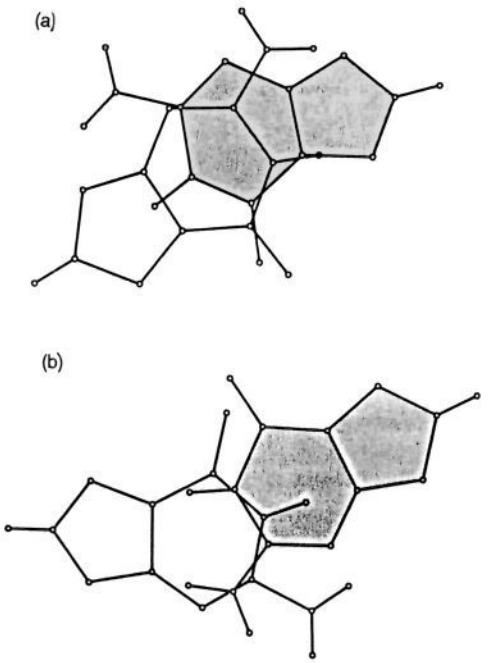

Figure 4. Intermolecular base–base stacking at the core of the tetrameric aggregate. Views are perpendicular to the 5′-guanine planes of molecules 1 and 2 in (a) and to the 3′-guanine planes of molecules 3 and 4 in (b). Guanine planes of molecules 2 and 4 are shaded. Hydrogen atoms are included.

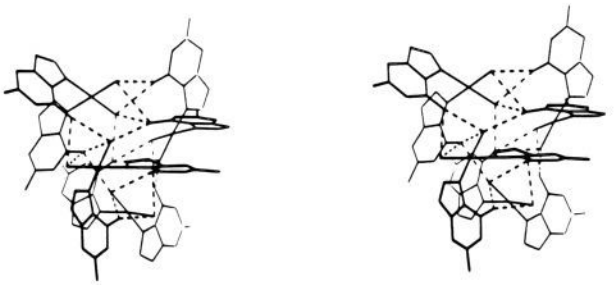

Figure 5. Stereoview of intermolecular hydrogen bonding at the core of the tetrameric aggregate. The sugar-phosphate backbone atoms are omitted for clarity. Hydrogen bonds are represented by dashed lines.

Rotations about the O5′B–C5′B bond (β_B) fall within the -ap range.[43] For molecules 1, 3, and 4 and conformation **a** of molecule 2, they are approximately 20°–40° more positive than the mean value seen in B-DNA crystals,[33,38b,39] but are near the value observed from fiber diffraction studies of A-DNA.[32] The value of 161° observed for conformation **b** of molecule 2 is closer to values found in crystals of both A- and B-DNA (Table III).

Although the broad range of values for torsion angle β_A (139°–207°) reflects the relative flexibility about the C5′A–O5′A bond of the free 5′-phosphate, torsion angle γ_A is confined to a smaller range (37°–72°), which implies more conformational rigidity about the C4′–C5′ bond. Torsion angles β_A and γ_A may be influenced by an intramolecular hydrogen bond which forms between a 5′-phosphate oxygen and an ammine ligand in at least three of the four platinum complexes. Shorter N···O (phosphate) distances are observed for molecules in conformational class I, while longer N···O (phosphate) distances are observed for molecules in class II (Table III). Values for γ_B exhibit a broader range than those for γ_A, consistent with disorder and high thermal motion within the 3′-deoxyribose residues.

Unit Cell Contents and Packing. At the core of the aggregate (Figure 1), the four platinum atoms lie at the vertices of a D_{2d} distorted tetrahedron having nonbonded Pt···Pt distances of 5.56 to 7.64 Å along its edges. The ammine ligands and the O6 atoms of the guanine bases point toward the center of the aggregate, while the sugar-phosphate backbones extend outward toward solvent channels and neighboring aggregates.

The tetrameric aggregate is stabilized by intermolecular base–base stacking interactions at its core and by a network of intermolecular hydrogen bonds at both the core and the periphery (Table IV). Stacking occurs between the 5′-guanines of molecules 1 and 2 and the 3′-guanines of molecules 3 and 4. Figure 4 displays these stacking interactions. Note that there is greater base–base overlap between molecules 1 and 2 than between molecules 3 and 4 and that in both interactions the N1–H group of one guanine lies above the ring π-electrons of the adjacent guanine.

Hydrogen-bonding interactions at the core occur mainly between ammine ligands and guanine O6 atoms of neighboring molecules (Figure 5). Additional hydrogen-bonding interactions may occur between the 3′-guanine O6 atom of molecule 2 and a 5′-phosphate proton of molecule 4 and between an ammine hydrogen of molecule 3 and a 5′-phosphate oxygen of molecule 2. Since the positions of hydrogen atoms bonded to nitrogen atoms of the ammine ligands, and to 5′-phosphate oxygen atoms, are unknown, hydrogen-bonding interactions at the core of the aggregate can only be proposed. A generous maximum donor··· acceptor distance of 3.30 Å was employed. In many instances, the ammine nitrogens are at hydrogen-bonding distances to four separate oxygen atoms, including the intramolecular phosphate oxygen, suggesting either the occurrence of bifurcated hydrogen bonds or that only the shortest donor–acceptor distances (Table IV) correspond to true hydrogen bonds.

Intermolecular hydrogen bonding at the periphery of the aggregate occurs between terminal 5′-phosphate oxygens and the N1-imino and exocyclic N2-amino hydrogen atoms of neighboring guanines (Figure 6). A hydrogen-bonding distance also occurs between an N2-amino hydrogen of molecule 1 and O5′A of molecule 2. Since the expected positions of N2-amino and N1-imino hydrogen atoms can be (and were) calculated from geometry, hydrogen-bonding interactions at the periphery are more certain than those at the core. Hydrogen···oxygen distances substantially smaller than the van der Waals distance of 2.6 Å have been accepted as indicative of hydrogen bonding, in keeping with the structural criteria for hydrogen bonding defined by Hamilton and Ibers.[45]

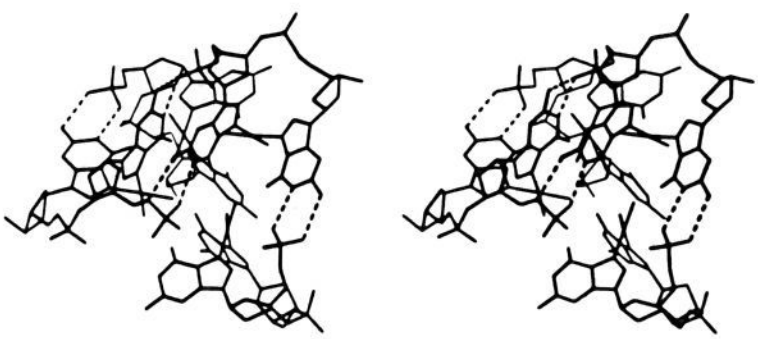

Figure 6. Stereoview of intermolecular hydrogen bonding at the periphery of the tetrameric aggregate. Hydrogen bonds are represented by dashed lines.

Within the unit cell, symmetry-related aggregates are largely separated from one another by water channels. Packing diagrams down all three crystallographic axes, which reveal the sizes of these channels and the interactions occurring between molecules of adjacent aggregates, are shown in Figure 7. Within the crystal, packing of aggregates is effected by 2-fold screw axes along the crystallographic *a* and *b* axes and by a C_2 axis along *c*. Aggregates are stacked on top of one another along *a*, creating a hydrophobic channel which runs between stacked bases through the cores of the aggregates. The largest water channels run parallel to the crystallographic *b* axis and are nearly 7 Å in diameter (Figure 7b). Smaller water channels run parallel to the *a* and *c* axes.

Along the vertical channels parallel to *b* in the view down *a*, intermolecular base pairing between guanines of adjacent tetrameric aggregates is visible. Specifically, two N2–H···N3 bonds occur between the 3′-guanines of molecules 1 and 2 to form a hydrogen-bonded pair, as illustrated below. Similar base pairing

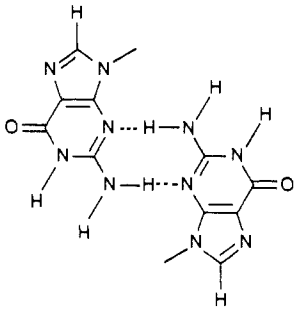

occurs between the 5′-guanines of two molecules 2 related by a C_2 axis along *c*. This interaction is visible within the vertical channel along *b* in Figure 7c. Such self-pairing of guanine via two N2–H···N3 hydrogen bonds has been observed in a number of crystal structures containing purine derivatives.[46] These and other proposed interaggregate hydrogen-bonding interactions are listed in Table V.

The positions of 27 water molecules (five at half-occupancy) and two glycine molecules were located in the asymmetric unit. Most of the water molecules occur in the first shell of hydration and are at hydrogen-bonding distances to phosphate oxygen atoms, ammine nitrogens, terminal O3′ atoms, and guanine ring heteroatoms. Some waters that have maintained good hydrogen bonding geometry during refinement have larger thermal parameters and may only partially occupy their positions. A few water molecules are not hydrogen bonded to any other located atoms but retained normal thermal parameters during refinement. Of the two located glycine molecules, only one is at hydrogen-bonding distances to other located atoms in the unit cell. The second glycine, isolated from other ordered atoms in a solvent channel, appeared in difference Fourier maps with a reasonable geometry.

Much of the solvent occurring in the water channels appears as a smear of electron density on difference maps and therefore seems to be disordered. The calculated density of the crystal based on the atoms which have been located is 1.282 g/cm^3.

The arrangement of ordered solvent and glycine molecules in the crystal lattice can be described by using the concept of nets.[47] Each net is comprised of a set of solvent molecules within hydrogen-bonding distance of each other and of donor or acceptor atoms on the platinum molecules. Distances up to 3.3 Å are accepted as possible hydrogen-bonding distances.

Ten ordered nets are observed in the asymmetric unit of the hydrated, glycinated crystals of *cis*-[Pt(NH$_3$)$_2${d(pGpG)}] (Table VI). The number of water molecules contained in each net ranges from one to six. Net 1, which contains just one water molecule, bridges two phosphate oxygen atoms within the same molecule. Nets 2 and 3, also containing just one water molecule, bridge atoms belonging to two or three molecules which are not necessarily within the same tetrameric aggregate. Nets containing more than one water molecule connect two or more platinum molecules in either an intraaggregate or interaggregate fashion.

Although the arrangement of water molecules in the asymmetric unit does not always follow the pseudo C_2 symmetry observed along *a* in Figure 1, some patterns in the hydration of the four platinum complexes have been observed. Water molecules form bridges between the two phosphate groups along the sugar phosphate backbone of each molecule. In molecules 2–4, these bridges consist of just one water. In molecule 4, two such bridges occur between oxygen atoms of the 5′-phosphate and OP2B. In molecule 1, two bridges, each consisting of two water molecules, occur between oxygen atoms of the 5′-phosphate and OP1B. For molecules 3 and 4 (class II), the heteroatoms of guanine are hydrated by ordered water molecules. Although no water molecules at hydrogen-bonding distances to the guanine heteroatoms of molecules 1 and 2 (class I) were located, one hydrogen bond does occcur between the nitrogen atom of glycine and O6B of molecule 1.

A relatively extensive net of ordered water molecules, net 9, links the base heteroatoms, N2A, N1A, and O6A of molecule 4 to phosphate oyxgen atoms, ammine ligands, and base heteroatoms of adjacent molecules. Included in this net is one four-membered ring made up entirely of water oxygens. Two other relatively extensive nets, 10 and 11, link heteroatoms of the 3′-guanines of molecules 3 and 4 with atoms in adjacent aggregates.

In net 11, which can be viewed in Figure 8, the carboxylate oxygens of glycine form hydrogen bonds to the 3′-guanine N1-imino and N2-amino hydrogens of molecule 4. It has been previously demonstrated that the N1 and N2 hydrogen atoms of guanine are in the correct geometry for bonding to the carboxylate functional group and that such hydrogen bonds form in both aqueous and organic media.[48] Hydrogen bonds also occur between glycine atoms and an ammine proton of molecule 3, an O6 atom of molecule 1, and water molecules. Water molecule 7, which is hydrogen-bonded to the glycine nitrogen atom, also bridges the 5′- and 3′-phosphate group along the sugar-phosphate backbone of molecule 3. Water molecule 19, which lies on a 2-fold axis along *c*, is hydrogen-bonded to carboxylate oxygen atoms from two C_2-related glycine molecules. Thus, net 11 links molecules 1, 3, and 4 to symmetry-related molecules in an adjacent tetrameric aggregate. A similar situation occurs in net 10, which links heteroatoms of the 3′-guanine of molecule 3 to oxygen atoms belonging to the 5′- and 3′-phosphate groups of molecule 4. Two C_2-related molecules of OW24 which hydrogen bond to N2B of molecule 3, also form hydrogen bonds to each other, linking symmetry-related molecules 3 and 4 of adjacent aggregates. Most of the atoms contained in nets 10 and 11 which link similar atoms of pseudo-2-fold-related molecules 3 and 4, respectively, are well-resolved and have relatively small thermal parameters. The fact that a glycine molecule was located in only one of these nets suggests that the arrangement of water and glycine molecules in the crystal lattice is at least one of the factors that breaks the potential C_2-symmetry along *a*.

Discussion

Crystallizations. Nucleic acids and their adducts are notoriously difficult to crystallize. There are two obvious approaches for obtaining crystals of a *cis*-DDP-oligonucleotide adduct. The first, which involves soaking nucleic acid crystals in solutions containing the drug, had already been attempted with limited success.[6,7] We decided to use the alternative method in which *cis*-DDP is allowed

(45) Hamilton, W. C.; Ibers, J. A. *Hydrogen Bonding in Solids*; W. A. Benjamin, Inc.: New York, 1968.

(46) (a) Sobell, H. M. *J. Mol. Biol.* **1966**, *18*, 1. (b) Mazza, F.; Sobell, H. M.; Kartha, G. *J. Mol. Biol.* **1969**, *43*, 407. (c) Labana, L. L.; Sobell, H. M. Proc. *Natl. Acad. Sci. U.S.A.* **1967**, *57*, 459. (d) Sakore, T. D.; Sobell, H. M.; Mazza, F.; Kartha, G. *J. Mol. Biol.* **1969**, *43*, 385. (e) O'Brien, E. J. *J. Mol. Biol.* **1963**, *7*, 107. (f) O'Brien, E. J. *Acta Crystallogr.* **1967**, *23*, 92. (g) Iball, J.; Wilson, H. R. *Nature (London)* **1963**, *198*, 1193. (h) Iball, J.; Wilson, H. R. *Proc. Roy. Soc. London* **1965**, *A288*, 418. (i) Broomhead, J. M. *Acta Crystallogr.* **1951**, *4*, 92.

(47) (a) Finney, J. L. *Phil. Trans. R.* Soc. *London* **1977**, *B278*, 3. (b) Jensen, L. H.; Watenpaugh, K. D. *Trans. Amer. Cryst. Assoc.* **1986**, *22*, 89.

(48) Lancelot, G.; Mayer, R. *FEBS Lett.* **1981**, *130*, 7 and references cited therein.

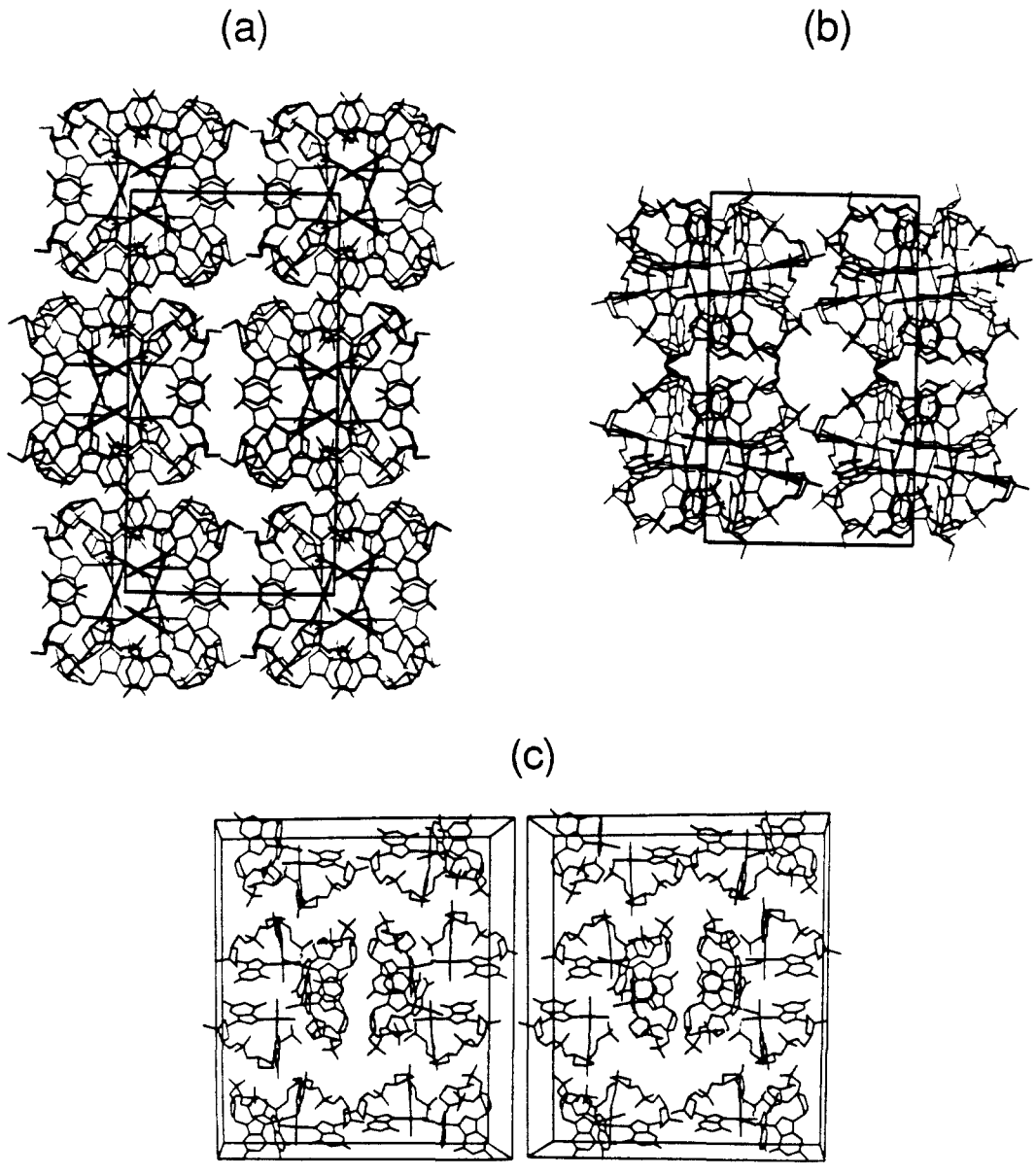

Figure 7. Packing diagrams of *cis*-[Pt(NH$_3$)$_2$\{d(pGpG)\}] viewed down the crystallographic axes. The contents of the unit cell are outlined: (a) view down *a*, (b) view down *b*, and (c) stereoview down *c*.

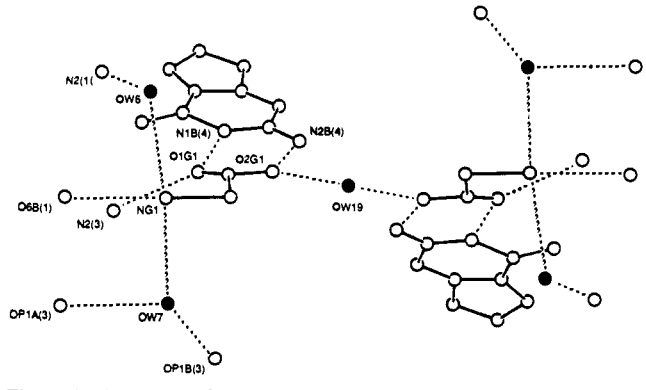

Figure 8. Structure of water net 11 (Table VI). Hydrogen bonds are represented by dashed lines. A crystallographic C_2 symmetry axis passes through OW19.

to react with an oligonucleotide in solution, followed by purification and crystallization of the resulting complex. This approach, using either single- or double-stranded oligonucleotides, seemed more likely to produce the desired results, since solution studies clearly demonstrate that DNA structure is significantly perturbed by reaction with *cis*-DDP.[11-16,49]

The dinucleotide, d(pGpG), is the smallest unit of DNA containing two adjacent guanosines, the major *cis*-DDP binding site, and a terminal 5′-phosphate. Manipulation of the charge on the 5′-phosphate of *cis*-[Pt(NH$_3$)$_2$\{d(pGpG)\}] (p$K_a \approx 6.7$)[11] facilitated separation and purification of the platinum complex by anion-exchange chromatography. Above neutral pH, the platinum complex is negatively charged, while at lower pH, the 5′-phosphate is monoprotonated and the platinum complex, neutral. This feature was also useful for crystallization purposes, since varying the pH of the buffer conditions resulted in two different species having crystallizing potential. Two crystalline forms of *cis*-[Pt(NH$_3$)$_2$\{d(pGpG)\}] were obtained at pH 4, where the complex is expected to be neutral. Attempts to grow crystals at neutral pH were unsuccessful.

The volume of the primitive unit cell is approximately half that of the C-centered cell (Table I). Specifically, $a \sim a', b \sim b'$, and $c \sim 1/2c'$, where a', b', and c' are the axes of the C-centered unit cell, indicating that the two crystal forms are related. The structure of the C-centered form has recently been solved, and the results will be presented elsewhere.[50]

(49) Sundquist, W. I.; Lippard, S. J.; Stollar, B. D. *Biochemistry* **1986**, *25*, 1520.

(50) Coll, M.; Wang, A. H.-J.; Sherman, S. E.; Gibson, D.; Lippard, S. J., to be submitted for publication.

Table III. Dinucleotide Geometry and Selected Intramolecular Distances[a]

(A) 5′-Nucleotide Torsion Angles[b]

torsion angle	molecule 1	molecule 2	molecule 3	molecule 4	A-DNA[c]	B-DNA[d]
χ_A	−90 (4)	−87 (4)	−138 (3)	−142 (4)	−160	−117
β_A	139 (3)	207 (2)	142 (2)	165 (3)	173	171
γ_A	58 (4)	72 (4)	56 (4)	37 (5)	52	54
δ_A	96 (4)	102 (3)	91 (5)	100 (5)	88	123
ϵ_A	−142 (3)	−145 (3)	−124 (4)	−133 (4)	−152	−169
ζ_A	−62 (3)	−62 (3)	−73 (4)	−64 (4)	−78	−108
ν_0	18 (4)	17 (3)	2 (4)	−7 (4)		
ν_1	−31 (4)	−29 (3)	−25 (4)	−26 (5)		
ν_2	30 (4)	29 (4)	40 (4)	42 (5)		
ν_3	−22 (4)	−18 (4)	−40 (4)	−44 (4)		
ν_4	3 (4)	2 (4)	28 (4)	34 (4)		

(B) 3′-Nucleotide Torsion Angles[b]

torsion angle	molecule 1	molecule 2	molecule 3	molecule 4	A-DNA[c]	B-DNA[d]
χ_B	−93 (5)	−118 (4)	−122 (4)	−127 (4)	−160	−117
α_B	−77 (5)	−82 (8) [177 (7)]	−59 (6)	−56 (5)	−62	−63
β_B	210 (4)	208 [161]	192 (5)	201 (4)	173	171
γ_B	24 (9)	61 [180]	43 (7)	40 (7)	52	54
δ_B	146 (7)	140 [166]	146 (6)	142 (5)	88	123
ν_0	−30 (5)	−35 [−22]	−56 (6)	−41 (5)		
ν_1	20 (8)	34 (6)	49 (5)	44 (5)		
ν_2	9 (7)	−16 [−22]	−27 (6)	−32 (6)		
ν_3	−27 (8)	−1 (11)	−1 (6)	16 (7)		
ν_4	34 (6)	20 [6]	35 (6)	14 (6)		

(C) Sugar Geometries[e]

item	molecule 1	molecule 2	molecule 3	molecule 4
P(5′)	−15	−16	18	25
Ψ(5′)	31	30	42	46
P(3′)	76	119 [143]	121	140
Ψ(3′)	38	33 [28]	52	42

(D) Selected Intramolecular Distances

distance	molecule 1	molecule 2	molecule 3	molecule 4
$P_A \cdots P_B$	6.18 (2)	5.79 (2)	5.67 (3)	5.61 (5)
N(ammine)···O(phosphate)	2.76 (4)	2.82 (3)	3.03 (3)	3.21 (4)

[a] Angles are in deg and distances are in Å. Numbers in parentheses are esd's where they could be calculated. Numbers in square brackets refer to the second disordered conformation **b** of molecule 2. [b] Torsion angles are defined as P-α-O5′-β-C5′-γ-C4′-δ-C3′-ε-O3′-ζ-P and χ for the glycosyl angle, O4′-C1′-N9-C4, with 0° at the eclipsed position and positive angles for clockwise rotation of the rear bond relative to the front bond. ν_0–ν_4 refer to endocyclic deoxyribose torsion angles.[40,41] [c] Mean values from the X-ray structure of the A-DNA octamer, d(GGTATACC), ref 36. [d] Mean values from the X-ray structure of the B-DNA dodecamer, d(CGCGAATTCGCG), ref 33a. [e] P and Ψ are defined according to the conventions in ref 40 and 42.

Effects of Platinum Binding on the Dinucleotide Structure. Several structural characteristics of the platinum-induced intrastrand d(GpG) crosslink had been established from solution NMR studies prior to this work. Binding of platinum to two guanine N7 atoms,[11-16] the head-to-head, anti orientations of the guanine bases,[11-14] the sugar puckers of the 5′- and 3′-nucleotides,[12-16] and the population distributions around the backbone torsion angles, γ, β, and ε,[12,13b] had all been revealed by ^{1}H NMR experiments. The X-ray crystal structure of *cis*-[Pt(NH$_3$)$_2${d(pGpG)}] provides significant details not only about the metrical aspects of these features but also about the orientations of the coordinated guanine bases and the important hydrogen-bonding interactions. These details will now be discussed.

In double-helical B-DNA, the base planes are stacked approximately 3.4 Å apart in a thermodynamically stable, parallel array.[41] Platinum coordination to adjacent guanosine N7 atoms in the major groove reduces the N7···N7 distance from 4.2 Å[51] to nearly 2.8 Å and forces the base planes to open up toward the minor groove. In *cis*-[Pt(NH$_3$)$_2${d(pGpG)}], the adjacent bases are completely destacked, with interplanar dihedral angles of 76.2 (5)° to 86.8 (6)°.

Geometric factors that influence the variations in Gua/Gua dihedral angles among the four molecules include the direction and degree of displacement of platinum from the guanine base planes and the direction and degree of rotation about the Pt–N7 bonds.[13b] A convention for describing displacement of platinum from the guanine base plane has been previously described.[8f] If platinum is displaced from the plane of one guanine base toward the cis N7 atom of a second coordinated base, the displacement is taken as positive, whereas if platinum is displaced away from the N7 atom of the second base, the displacement is said to be negative. Three situations can arise in the case of platinum bound to two guanine bases (designated +,+; +,−; or −,−), corresponding to increasing dihedral angles between the two base planes. The four *cis*-[Pt(NH$_3$)$_2${d(pGpG)}] molecules follow this trend. Displacements of platinum in molecule 1 are +,+, while the other molecules all have +,− displacements (Table S6). The result is a smaller Gua/Gua dihedral angle for molecule 1 (Table II). The magnitudes of displacements in the positive or negative directions are also important, as can be appreciated by inspecting the relative displacements and Gua/Gua dihedral angles of molecules 2–4 in Tables II and S6.

The base/PtN$_4$ dihedral angles also have a geometric influence on the magnitudes of the base/base dihedral angles. When both bases rotate in the same direction relative to an orientation perpendicular to the PtN$_4$ plane, the base/base dihedral angle is effectively decreased. If they rotate in opposite directions, the dihedral angle is effectively increased. The size of the effect depends on the relative magnitudes of the two rotations. The guanines rotate in opposite directions in molecule 1, maximizing the distance between their bulky constituents and closing down the intramolecular C8···C8 distance. When viewed down the

(51) Arnott, S.; Smith, P. J. C.; Chandrasekaran, R. In *CRC Handbook of Biochemistry and Molecular Biology, Nucleic Acids*; Fasman, G. D., Ed.; CRC Press: Ohio, 1976; Vol. II, p 411.

Table IV. Intermolecular Stacking and Hydrogen Bonding Interactions within the Tetrameric Aggregate[a]

(A) Stacking Interactions[b]

	distance
5′-Guanine(1)···5′-Guanine(2)	3.29 Å
3′-Guanine(3)···3′-Guanine(4)	3.32 Å

(B) Possible Hydrogen Bonds at Core

donor atom(D)	acceptor atom(A)	D···A (Å)	donor atom(D)	acceptor atom(A)	D···A (Å)
N1(1)	O6A(2)	3.12 (3)	N1(3)	O6B(1)	2.97 (4)
N1(1)	O6A(4)	2.97 (4)	N2(3)	O6B(1)	2.72 (4)
N1(1)	O6B(4)	3.10 (3)	N2(3)	O6A(1)	3.02 (3)
N2(1)	O6A(4)	3.15 (3)	N2(3)	O6B(4)	3.06 (3)
N2(1)	O6B(4)	3.21 (3)	N1(4)	O6A(2)	3.02 (3)
N1(2)	O6A(1)	2.97 (3)	N1(4)	O6B(2)	2.99 (4)
N1(2)	O6A(3)	2.95 (4)	N2(4)	O6A(2)	3.07 (4)
N1(2)	O6B(3)	3.15 (3)	N2(4)	O6B(2)	2.77 (4)
N2(2)	O6A(3)	3.07 (3)	OP1A(4)	O6B(2)	3.23 (4)
N2(2)	O6B(3)	3.07 (3)	N1(3)	OP1A(2)	2.98 (3)
N1(3)	O6A(1)	2.94 (3)			

(C) Proposed Hydrogen Bonds at Periphery

D	H	A	H···A (Å)	D···A (A)	∠D–H···A (deg)
N1A(1)	H1A(1)	OP1A(2)	1.81 (3)	2.75 (3)	165 (3)
N2A(1)	H2A1(1)	O5′A(2)	2.09 (3)	3.03 (3)	173 (3)
N1B(1)	H1B(1)	OP1A(3)	1.88 (3)	2.82 (3)	167 (3)
N2B(1)	H2B1(1)	OP2A(3)	2.04 (4)	2.96 (4)	162 (3)
N1A(2)	H1A(2)	OP3A(1)	1.75 (4)	2.61 (4)	149 (3)
N2A(2)	H2A1(2)	OP3A(1)	2.12 (4)	2.87 (4)	135 (3)
N1B(2)	H1B(2)	OP1A(4)	1.77 (4)	2.69 (4)	162 (3)
N2B(2)	H2B1(2)	OP2A(4)	2.15 (6)	3.12 (6)	178 (4)

[a] For atom labels and guanine planes, numbers in parentheses designate molecules 1–4. [b] Stacking distances were calculated by averaging the distances of every atom in both bases to the best plane of the opposite base.

Table V. Proposed Interaggregate Hydrogen Bonding Interactions[a]

D	H	A	H···A (Å)	D···A (Å)	∠D–H···A (deg)
N2B(1)	H2B2(1)	N3B(2)	2.24 (4)	3.17 (4)	164 (3)
N2B(2)	H2B2(2)	N3B(1)	2.00 (5)	2.94 (5)	171 (4)
N2A(2)	H2A2(2)	N3A(2)	2.09 (4)	3.03 (4)	163 (3)
N2B(3)	H2B1(3)	N3B(4)	2.49 (5)	3.39 (5)	157 (4)
N2A(4)	H2A1(4)	OP3A(2)	2.31 (5)	3.11 (5)	144 (4)
N2B(4)	H2B2(4)	N3B(3)	2.35 (5)	3.25 (5)	158 (3)
O3′B(1)[b]		OP2A(4)[b]		2.81 (8)	
O3′B(2)[b]		OP2A(3)[b]		2.80 (7)	

[a] For atom labels, numbers in parentheses designate molecules 1–4. [b] For these atoms, it is unclear which is the donor atom and which is the acceptor atom.

N7–Pt vector, the 5′-guanine rotates in a clockwise direction, while the 3′-guanine rotates in a counterclockwise direction. In molecules 2, 3, and 4, both bases rotate in the same direction when viewed down the respective N7–Pt vectors (Figure 3).

As a guanine base rotates away from perpendicularity toward the PtN$_4$ coordination plane, the distance between its O6 atom and a coordinated ammine ligand may decrease. In molecules 3 and 4, the 3′-Gua/PtN$_4$ angles are 58°–60°, resulting in N(ammine)···O6 distances of ~3.1 Å (Table II). In several X-ray structural studies of amine complexes of platinum bound to 6-oxopurine bases, researchers have observed similar or smaller base/PtN$_4$ dihedral angles (values of 46°–63° for either the angle or its supplement) and similar or shorter distances between the O6 atom of the base and a cis amine nitrogen (2.86–3.13 Å), suggesting the presence of a hydrogen bond.[9,10,52,53] By using computer graphics modelling, we have observed that rotation of NH$_3$ about the Pt–N(ammine) bond in molecule 3 allows an optimal H(ammine)···O6 distance of 2.26 Å and an N–H···O6 angle of 148°, which implies that interligand H(ammine)···O6 hydrogen bonds in molecules 3 and 4 are weak, at best.[45] Moreover, the ammine nitrogen atoms of molecules 3 and 4 are at hydrogen-bonding geometry to guanine O6 atoms of three (molecule 3) or two (molecule 4) neighboring molecules. It is therefore likely that intermolecular interactions are more important than intramolecular interactions in this instance. In molecules 1 and 2, the 5′-Gua/PtN$_4$ dihedral angles are 111°. Here, the

(52) Orbell, J. D.; Wilkowski, K.; de Castro, B.; Marzilli, L. G.; Kistenmacher, T. J. *Inorg. Chem.* **1982**, *21*, 813, and references cited therein.
(53) Admiraal, G.; van der Veer, J. L.; deGraff, R. A. G.; den Hartog, J. H. J.; Reedijk, J. *J. Am. Chem. Soc.* **1987**, *109*, 592. Coordinates of the X-ray structure were kindly supplied to us by J. Reedijk.

Table VI. Proposed Hydrogen Bonding Interactions of Water and Glycine Molecules[a]

net no.	interaction	distance (Å)	interaction	distance (Å)
1	OW1···OP2A(4)	2.41 (8)[b]	OW1···O5′A(4)	3.31 (7)
	OW1···OP1B(4)	3.2 (1)		
2	OW8···OP2A(1)	3.10 (7)	OW8···N1(4)	3.15 (6)
3	OW14···OP3A(2)	2.70 (4)	OW14···N3A(4)	3.01 (4)
	OW14···OP3A(3)	2.66 (4)		
4	OW25···OP3A(1)	2.7 (1)		
5	OW23···OP1B(1)	2.61 (8)		
6	OW9···OP2A(2)	2.62 (3)	OW9···OW22	2.88 (6)
	OW9···OP1B(2)	2.70 (4)	OW22···N1A(3)	3.26 (7)
7	OW26···OP2B(4)	3.1 (1)	OW27···OP2B(2)	2.7 (2)
	OW26···OW27	3.2 (2)	OW27···OP2B(4)	2.6 (2)
8	OW13···OP2A(1)	2.36 (6)	OW13···N3A(3)	3.14 (6)
	OW13···OW18	2.71 (8)	OW18···OP1B(1)	2.63 (8)
9	OW10···OP1B(1)	2.75 (5)	OW12···O6A(4)	3.03 (5)
	OW10···OW12	2.71 (6)	OW12···N2A(3)	2.93 (6)
	OW10···OW21	2.8 (1)	OW12···OW15	3.14 (9)
	OW12···OP1A(1)	2.54 (6)	OW15···N2(1)	3.07 (8)
	OW15···N1A(4)	2.99 (9)	OW16···OP1B(2)	2.84 (8)
	OW15···O6A(4)	3.12 (8)	OW16···N2A(4)	2.85 (8)
	OW15···OW16	2.9 (1)	OW23···OP1B(1)	2.61 (8)
	OW15···OW21	3.0 (1)		
10	OW2···OW3	2.87 (5)	OW4*···N1B(3)	2.92 (6)
	OW2···OP1A(4)	2.90 (5)	OW4*···N2B(3)	3.18 (6)
	OW2···OP2B(4)	2.92 (8)	OW4*···OW24	2.41 (9)[b]
	OW2···O5′A(4)	3.16 (5)	OW5*···N1B(3)	3.23 (7)
	OW3*···OW4*	2.83 (7)	OW24···OW24	3.3 (1)
	OW3*···OW5*	1.77 (8)[c]	OW24···O3′B(4)	2.83 (8)
	OW3*···N2(4)	2.94 (5)	OW24···N2B(3)	3.28 (9)
	OW4*···OW5*	1.21 (9)[c]		
11	OW6···N2(1)	2.94 (5)	OW19···O2G1	2.94 (8)
	OW6···NG1	3.04 (8)	O1G1···N1B(4)	2.78 (5)
	OW7···OP1A(3)	3.04 (4)	O1G1···N2(3)	2.81 (4)
	OW7···OP1B(3)	2.76 (6)	O2G1···N2B(4)	2.81 (6)
	OW7···NG1	2.93 (7)	NG1···O6B(1)	3.14 (7)
	OW7···O5′A(3)	2.95 (4)		

[a] OW means water oxygen. O1GL, O2GL, and NGL are the respective oxygen and nitrogen atoms of glycine 1. Numbers in parentheses after atom labels refer to molecules 1–4. Asterisks designate water molecules at half-occupancy. [b] The large error on this value obviates concern about the short distance. [c] These distances are artificial, owing to the disorder, and both sites would not be occupied in any one unit cell.

Table VII. Close Contacts between Hypothetical Axial Ligands Added to the Structure of *cis*-[Pt(NH$_3$)$_2$\{d(pGpG)\}] and Atoms of the Dinucleotide[a]

added ligands	molecule 1[b]	molecule 2[b]	molecule 3[b]	molecule 4[b]
OH1 and OH2	OH1···O6B (1.94)	OH1···O6B (1.82)	OH1···O6B (2.62)	OH1···O6B (2.46)
	OH1···O6A (2.11)	OH1···O6A (2.45)	OH1···O6A (1.95)	OH1···O6A (1.91)
Cl$_1$ and Cl$_2$	Cl1···O6B (1.80)	Cl1···O6B (1.68)	Cl1···O6B (2.58)	Cl1···O6B (2.41)
	Cl1···O6A (2.03)	Cl1···O6A (2.37)	Cl1···O6A (1.80)	Cl1···O6A (1.78)
	Cl2···H8B1 (2.48)	Cl2···H8B2 (2.49)	Cl2···H8B3 (2.50)	Cl2···H8B4 (2.64)
	Cl2···H8A1 (2.60)	Cl2···H8A2 (2.32)	Cl2···H8A3 (2.45)	Cl2···H8A4 (2.56)

[a] For details, see text. [b] Distances are measured in Å.

long N(ammine)···O6 distances of 3.3–3.5 Å preclude hydrogen bonding.

In order to understand how the dinucleotide structure adjusts to accommodate the extensive unstacking of the guanine bases in *cis*-[$Pt(NH_3)_2${d(pGpG)}], its backbone torsion angles and sugar conformations have been compared to those from X-ray diffraction studies of A- and B-DNA (vide supra). Taken together, the backbone torsion angles of the four molecules do not fit neatly into either of these two structural categories. The C3′-endo/C2′-exo sugar puckers of the 5′-nucleotides are more characteristic of A-DNA than of B-DNA. The result is compressed intramolecular phosphorus···phosphorus distances of 5.61 (5)–6.18 (2) Å (Table III), compared to the average phosphorus···phosphorus distance of 6.7 Å found in the X-ray structure of a B-DNA dodecamer.[33a] The phosphorus···phosphorus distances in *cis*-[$Pt(NH_3)_2${d(pGpG)}] are more similar to the average phosphorus···phosphorus distance of 6.0 Å found in crystals of A-DNA oligonucleotides,[26b,36] The observed pattern of phosphate hydration, in which one or two water molecules form bridges between oxygen atoms belonging to adjacent phosphate groups on the same strand, is also characteristic of A-DNA.[54] Moreover, backbone torsion angles of the 5′-guanosine of platinated d(pGpG), δ_A, ϵ_A, and ζ_A, are more characteristic of A-DNA than B-DNA (Table III). Although the values of ϵ_A and ζ_A appear to be correlated in a way similar to B-DNA, where higher values of ζ occur with lower values of ϵ,[33b,38b,39] a plot of ϵ_A versus ζ_A for the four molecules of *cis*-[$Pt(NH_3)_2${d(pGpG)}] is significantly displaced from the same plot for B-DNA (Figure 9). Indeed, the points on this plot fall much closer to the points observed for A-DNA, where no apparent correlation between ϵ and ζ was observed.[36]

The backbone conformations of the 3′-guanosines in *cis*-[$Pt(NH_3)_2${d(pGpG)}] are more difficult to categorize. The relatively large temperature factors and poor metrical parameters of the 3′-sugar ring atoms suggest that there may be a distribution between C2′-endo and C3′-endo puckers in the solid state, similar to the temperature-dependent distribution between C2′-endo (70–80%) and C3′-endo conformations observed in solution studies of *cis*-[$Pt(NH_3)_2${d(GpG)}]-containing oligonuleotides.[12,13b,14b] The two disordered conformations at the 3′-end of molecule 2 do not reflect such a distribution, although all of the disordered atoms in this molecule may not have been located (vide supra).

An obvious difference between the structures of the platinated dinucleotides and unperturbed DNA occurs in the glycosyl torsion angles, χ. In unperturbed DNA, this angle is related to sugar pucker.[55] In A-DNA, for example, where only the C3′-endo conformation exists, χ has been observed to span a small range (~30°) centered around −160°.[26b,36] In B-DNA, the value of χ is strongly correlated to torsion angle δ and thus to the deoxyribose ring pucker.[33b] When the value of δ is ~145°, typical of the C2′-endo conformation, the value of χ lies ~−100°. When the value of δ is around 90°, typical of the C3′-endo sugar pucker, the value of χ changes to ~−140°. Inspection of the χ values in the four molecules of *cis*-[$Pt(NH_3)_2${d(pGpG)}] (Table III) reveals that the B-DNA correlation does not hold for the platinated dinucleotides. At the 5′-end, where the average value of δ is 97°, the range of χ values extends from −87 (4)° to −142 (4)°. At the 3′-end, where the average value of δ is 144°, χ ranges from −93 (5)° to −127(4)°. Moreover, the difference between the two values of χ in any given molecule does not exceed 31°. The broad ranges of χ values at the 5′- and 3′-ends of the four molecules reflect a certain amount of flexibility in the conformation of *cis*-[$Pt(NH_3)_2${d(pGpG)}], as do the two disordered conformations of molecule 2. This conformational flexibility can be viewed in Figure 10, where the four crystallographically independent molecules are superimposed.

An important feature of the X-ray structure of *cis*-[$Pt(NH_3)_2${d(pGpG)}] is a hydrogen bond which forms between a terminal 5′-phosphate oxygen and an ammine ligand in at least

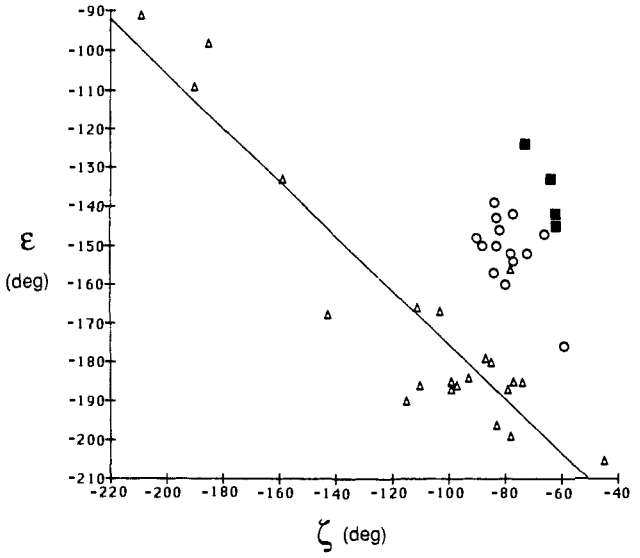

Figure 9. Plot of ϵ versus ζ, comparing values for B-DNA (Δ), A-DNA (○), and *cis*-[$Pt(NH_3)_2${d(pGpG)}] (■). Data from X-ray crystal structures of B-DNA and A-DNA oligonucleotides were taken from ref 33b and 36, respectively.

three of the four molecules (Table III). By using computer graphics modelling, we have found that rotation of NH_3 about the Pt–N(ammine) bond of molecule 1 allows an optimal H(ammine)···O(phosphate) distance of 1.6 Å and an N–H···O angle of 170°, characteristic of strong hydrogen bonding.[45] This interaction was originally observed by molecular mechanics calculations on platinated single- and double-stranded oligonucleotides,[56] which implies that it could occur when platinum is bound to adjacent guanines in duplex DNA. Recently, evidence for an ammine···phosphate hydrogen bond in solution has been found by NMR spectroscopic studies of an ethylenediamine complex of 5′-AMP.[57] Such hydrogen bonding may be an important feature of clinically useful platinum anticancer drugs, stabilizing their DNA adducts and leading ultimately to tumor-growth inhibition.

Because *cis*-[$Pt(NH_3)_2${d(pGpG)}] is comprised of only two nucleotides, it is impossible to determine its overall helicity. Depending on the angle from which the structure is viewed, it could equally well fit into both left-handed and right-handed DNAs. In Figure 11, the structures of d(pGpG) in class I and class II conformations of *cis*-[$Pt(NH_3)_2${d(pGpG)}] are compared to that of right-handed B-DNA. These diagrams demonstrate the local structural consequences that could occur upon platinum binding to DNA in its normal B-conformation. As has been already described, the most prominent perturbations to the sugar-phosphate backbone occur at the 5′-end of the molecule. In addition, tipping of both guanine base planes relative to the parallel, stacked array in B-DNA can be clearly observed. In conformational class I of *cis*-[$Pt(NH_3)_2${d(pGpG)}], the 5′-guanine is tilted out of the B-DNA base plane to a greater extent than the 3′-guanine. In conformational class II, both guanine planes are tipped out of the B-DNA base planes by nearly the same amount.

Comparisons with Other Structural Studies of Platinated DNA Fragments. The X-ray structure of *cis*-[$Pt(NH_3)_2${d(CpGpG)}] at 1.8 Å resolution has recently been reported.[53] This molecule crystallizes with three crystallographically independent molecules in the asymmetric unit. With structures at atomic resolution of seven independent molecules containing the d(GpG)-platinum crosslink now in hand, it is both possible and of interest to make some comparisons.

The 5′- and 3′-sugar puckers in all molecules are similar, as are the dihedral angles between the destacked guanine planes. The

(54) Saenger, W.; Hunter, W. N.; Kennard, O. *Nature (London)* **1986**, *324*, 385.
(55) Arnott, S. *Prog. Biophys. Mol. Biol.* **1970**, *21*, 267.
(56) (a) Kozelka, J.; Petsko, G. A.; Lippard, S. J.; Quigley, G. J. *J. Am. Chem. Soc.* **1985**, *107*, 4079. (b) Kozelka, J.; Petsko, G. A.; Quigley, G. J.; Lippard, S. J. *Inorg. Chem.* **1986**, *25*, 1075. (c) Kozelka, J.; Archer, S.; Petsko, G. A.; Lippard, S. J.; Quigley, G. J. *Biopolymers* **1987** *26*, 1245.
(57) Reily, M. D.; Marzilli, L. G. *J. Am. Chem. Soc.* **1986**, *108*, 6785.

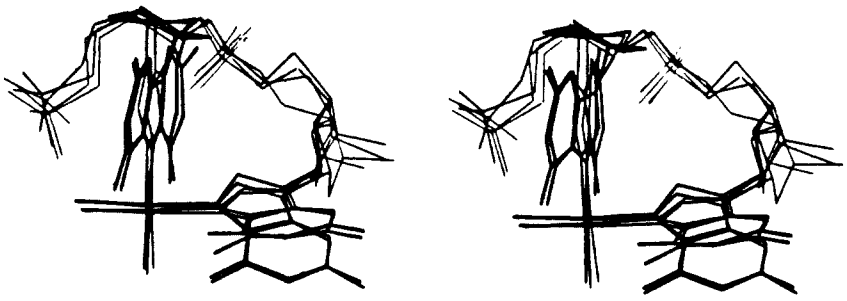

Figure 10. Stereoview of molecules 1–4 of *cis*-[Pt(NH$_3$)$_2${d(pGpG)}], superimposed on one another by using the molecular graphics program, HYDRA.[28] To produce the superposition, molecule 2 was least-squares fit to molecule 1, molecule 4 was least-squares fit to molecule 3, and molecule 3 was least-squares fit to molecule 2. Conformation **b** was used for molecule 2 to show the maximum structural deviation.

phosphorus···phosphorus distances in all molecules are shortened relative to that in B-DNA, with values ranging from 5.54–5.92 Å in the three crystallographically independent molecules of *cis*-[Pt(NH$_3$)$_2${d(CpGpG)}] (cf. Table III). The Gua/PtN$_4$ dihedral angles, however, in all three d(CpGpG)-platinum molecules are quite different from the values found in either the class I or class II conformations of *cis*-[Pt(NH$_3$)$_2${d(pGpG)}]. While the 3′-Gua/PtN$_4$ angles of the d(CpGpG) structures are all near 90°, the 5′-Gua/PtN$_4$ angles are more exaggerated ranging from 124° to 130°. These values give rise to shorter N(ammine)···O6 distances (2.94–3.03 Å) than those in the four *cis*-[Pt(NH$_3$)$_2${d(pGpG)}] molecules. The values of χ in *cis*-[Pt(NH$_3$)$_2${d(CpGpG)}], like those in *cis*-[Pt(NH$_3$)$_2${d(pGpG)}], are not correlated with the sugar pucker. Although the difference between the 5′-χ, −76 (4)°, and 3′-χ, −91 (5)° values of molecule 2 of *cis*-[Pt(NH$_3$)$_2${d(CpGpG)}] falls within the range observed in the platinated d(pGpG) structure, the differences between the values of 5′-χ and 3′-χ of molecules 1, −69 (5)°; −116 (6)°, and 3, −74 (7)°; −119 (7)°, of *cis*-[Pt(NH$_3$)$_2${d(CpGpG)}] are larger, 47° and 45°, respectively. In all seven molecules, there is a correlation between χ values at the 5′-end and PtN$_4$/5′-Gua dihedral angles. Specifically, more negative values of 5′-χ occur with smaller PtN$_4$/5′-Gua angles. No such correlation exists between χ values and PtN$_4$/Gua dihedral angles at the 3′-ends of the molecules.

Although molecule 2 of the *cis*-[Pt(NH$_3$)$_2${d(CpGpG)}] structure has very similar torsion angles to those found in molecules 1, 3, and 4 and conformation **a** of molecule 2 in the present structure, molecules 1 and 3 (molecule 3 was less accurately determined[53]) of the *cis*-[Pt(NH$_3$)$_2${d(CpGpG)}] structure have unusual values of torsion angles α_B, −112 (7)° and 145 (10)°, respectively, and γ_B, 99 (10)° and 189 (10)°, respectively. Indeed, α_B and γ_B of molecule 3 are somewhat similar to those in conformation **b** of molecule 2 in *cis*-[Pt(NH$_3$)$_2${d(pGpG)}]. The trans conformations for γ_B found in the latter molecules are not totally unexpected. In solution, this torsion angle adopts the gauche$^+$ conformation for 65–79% of the population, depending on temperature, in *cis*-[Pt(NH$_3$)$_2${d(CpGpG)}] and *cis*-[Pt(NH$_3$)$_2${d(GpG)}].[12,13b] For *cis*-[Pt(NH$_3$)$_2${d(CpGpG)}], the conformation of the remaining population was identified as trans.[13b]

No H(ammine)···O(phosphate) hydrogen bonding similar to that seen in the X-ray structure of platinated d(pGpG) occurs in the X-ray structure of *cis*-[Pt(NH$_3$)$_2${d(CpGpG)}]. The 5′-cytosine base, shown by NMR studies to stack on the adjacent guanosine in solution, is destacked in all three molecules in the solid state. This result presumably arises from intermolecular hydrogen bonding and/or stacking interactions. Such solid-state forces may also orient the cytosine 3′-phosphate away from the platinum coordination plane and out of range for hydrogen bonding to a coordinated ammine group.

Comparisons between the X-ray structure of *cis*-[Pt(NH$_3$)$_2$-{d(pGpG)}] and the predominant structure of the related complex *cis*-[Pt(NH$_3$)$_2${d(GpG)}] obtained in solution by NMR and model building[12] revealed the backbone conformational angles of the two structures to be very similar.[17] The ^{31}P NMR spectrum of *cis*-[Pt(NH$_3$)$_2${d(GpG)}] is typical of helical DNA, which implies gauche/gauche conformations of the interguanine phosphodiester torsion angles ζ and α,[12] similar to those found in molecules 1, 3, and 4 and conformation **a** of molecule 2 in the X-ray structure of *cis*-[Pt(NH$_3$)$_2${d(pGpG)}]. Interestingly, a 0.9–1.5 ppm downfield shift of the interguanine phosphorus resonance has been observed in the ^{31}P NMR spectra of *cis*-[Pt(NH$_3$)$_2${d(CpGpG)}][13] and all longer oligonucleotides and DNAs studied containing the intrastrand platinated d(GpG) crosslink.[15,16b,58] The origins of this downfield shift are not yet understood, but it could arise from a change in ζ and α torsion angles away from the typical gauche/gauche to trans/gauche or gauche/trans conformations as well as from a decrease in the phosphodiester O(3′)–P–O(5′) angle.[59] The presence of a base 5′ to the platinated guanosines may be necessary in order for the unusual geometry around the interguanine phosphorus and downfield ^{31}P NMR chemical shift to occur.[13b] No significant alteration in the O(3′)–P–O(5′) angle has been observed in the X-ray structure of *cis*-[Pt(NH$_3$)$_2${d(pGpG)}]. Conformation **b** of molecule 2 indicates, however, that angle α_B can undergo an unusual conformational change when platinum binds to neighboring guanines, even in the absence of a 5′-base.

The X-ray structures of three structurally different salts of *cis*-[Pt(NH$_3$)$_2$(9-ethylguanine)$_2$]$^{2+}$ containing head-to-head orientations of the guanine bases have been published.[10] In these structures having unlinked guanines, base/base dihedral angles are slightly smaller, ranging from 68°–78°. As discussed previously, this result is partly due to the relative values of the 5′-Gua/PtN$_4$ and 3′-Gua/PtN$_4$ dihedral angles. The chloride and sulfate salts of *cis*-[Pt(NH$_3$)$_2$(9-ethylguanine)$_2$]$^{2+}$ have 5′-Gua/PtN$_4$ and 3′-Gua/PtN$_4$ dihedral angles (Cl^- = 131°, 105°; SO_4^{2-} = 80°, 51°) similar to, but more exaggerated than, the dihedral angles seen in class I and class II molecules, respectively, of *cis*-[Pt(NH$_3$)$_2${d(pGpG)}]. Moreover, the C9′···C9′ distances for the salts (6.25 and 6.45 Å, respectively) are within the range of corresponding C1′···C1′ distances (6.05–6.79 Å) in the present structure. On the other hand, the 5′- and 3′-Gua/PtN$_4$ dihedral angles of the [Pt(CN)$_4$]$^{2-}$ salt of *cis*-[Pt(NH$_3$)$_2$(9-ethylguanine)$_2$]$^{2+}$ are nearly the same (119° and 117°, respectively), resulting in a long, 7.59 Å C9′···C9′ distance.[10]

From these comparisons, it can be concluded that unlinked guanines adopt a greater variety of orientations relative to the guanine bases in *cis*-[Pt(NH$_3$)$_2${d(pGpG)}], which are restricted by the conformation of the 17-membered chelate ring that includes the DNA backbone. It is difficult to predict, based on the present structure, whether Gua/Gua and Gua/PtN$_4$ angles similar to those in the chloride and sulfate salts of *cis*-[Pt(NH$_3$)$_2$(9-ethylguanine)$_2$]$^{2+}$ could occur when platinum binds to DNA.

Structural Aspects of *cis*-[Pt(NH$_3$)$_2${d(pGpG)}] and the Question of Octahedral versus Planar Platinum Drugs. What can be learned from the molecular geometry of *cis*-[Pt(NH$_3$)$_2${d(pGpG)}] about the structures of other platinum anticancer drugs bound to DNA?

(58) (a) den Hartog, J. H. J.; Altona, C.; van Boom, J. H.; Reedijk, J. *FEBS Lett.* **1984**, *176*, 393. (b) Marzilli, L. G.; Reily, M. D.; Heyl, B. L.; McMurray, C. T.; Wilson, W. D. *FEBS Lett.* **1984**, *176*, 389. (c) Reily, M. D.; Marzilli, L. G. *J. Am. Chem. Soc.* **1985**, *107*, 4916.

(59) (a) Gorenstein, D. G.; Findlay, J. B.; Momii, R. K.; Luxon, B. A.; Kar, D. *Biochemistry* **1976**, *15*, 3796. (b) Haasnoot, C. A. G.; Altona, C. *Nucleic Acids Res.* **1979**, *6*, 1135. (c) Gorenstein, D. G. In *Phosphorus-31 NMR*; Academic Press: Orlando, FL, 1984; Chapter 8.

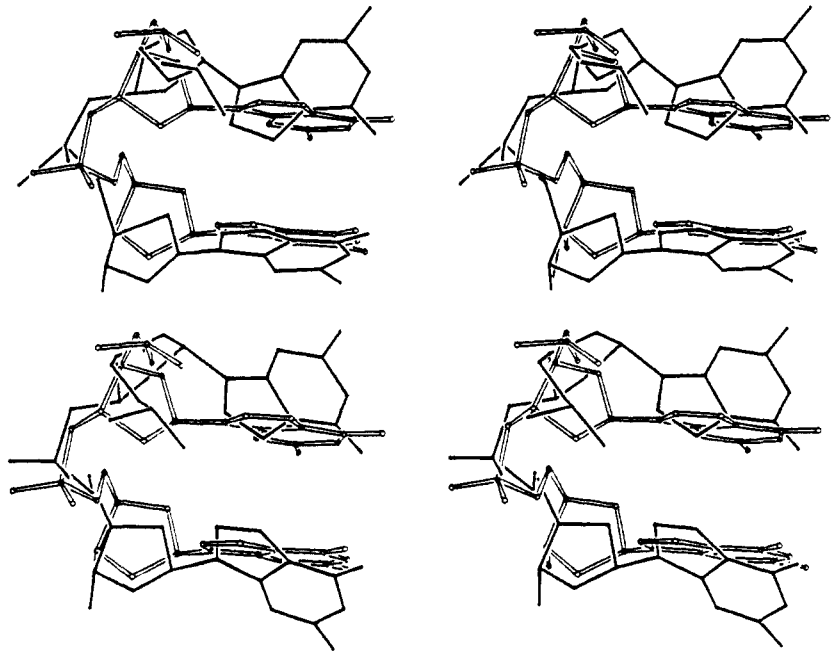

Figure 11. Comparisons between the B-DNA dinucleotide, d(pGpG) generated from fiber diffraction coordinates (ref 51), and Class I (molecule 1, top stereoview) and Class II (molecule 4, bottom stereoview) conformations of *cis*-[Pt(NH$_3$)$_2$[d(pGpG)]]. Pt, N1, and N2 were removed from each set of *cis*-[Pt(NH$_3$)$_2$[d(pGpG)]] coordinates, and the remaining atoms were least-squares fit to d(pGpG). In both views, the B-DNA dinucleotide has open bonds.

One of the first platinum compounds found to be active against tumors was the octahedral complex, *cis*-[Pt(NH$_3$)$_2$Cl$_4$].[60] Another octahedral platinum complex, *cis,cis,trans*-[Pt(NH$_2$CH(CH$_3$)$_2$)$_2$Cl$_2$(OH)$_2$], or iproplatin, is currently undergoing clinical trials.[61] Yet, the reactions of Pt^{IV} complexes with DNA are more poorly understood than those of square-planar Pt^{II} complexes. There is some question as to whether or not Pt^{IV} complexes are reduced in vivo prior to reaction with DNA.[62] As pointed out previously, it is possible that, depending on the ligands involved, both Pt^{IV} and reduced Pt^{II} species react with DNA in cells treated with octahedral platinum drugs.[63] In order to assess how well an octahedrally coordinated metal might fit into the intrastrand crosslinked d(GpG) structure described here, two hypothetical ligands, Cl$^-$ or OH$^-$, were introduced into the platinum coordination sphere perpendicular to the PtN$_4$ coordination planes of molecules 1–4. By using molecular graphics, close contacts between these ligands and atoms of the dinucleotide were evaluated for all four molecules. Specifically, for both Cl$^-$ (Pt–Cl = 2.30 Å) and OH$^-$ (Pt–OH = 2.00 Å) coordination, one of the added ligands formed unacceptably close contacts with O6 atoms of both guanine bases (Table VII). In the case of Cl$^-$ coordination, the second added ligand is sterically too close to H8 atoms of the guanine bases. The results of this exercise indicate that the kinds of conformations observed for d(pGpG) in the X-ray structure of *cis*-[Pt(NH$_3$)$_2$[d(pGpG)]] could not occur for binding of an octahedral complex to DNA. Whether or not significant departures from this geometry could occur to accommodate an intrastrand crosslinked *cis*-[Pt(NH$_3$)$_2$X$_2$[d(GpG)]] unit in an oligonucleotide adduct of octahedral Pt^{IV} is unknown.

Biological Relevance. Both the single-stranded nature of *cis*-[Pt(NH$_3$)$_2$[d(pGpG)]] and the effects of packing forces within the crystal lattice must be considered in assessing the likely relevance of the structure described here to the structural perturbations that occur when the *cis*-{Pt(NH$_3$)$_2$}$^{2+}$ moiety binds to adjacent guanines on DNA. The similarities between the most prevalent sugar-phosphate backbone geometry in the solid-state structure and that in solution[17] suggest that crystal packing effects are minimal. The occurrence of four crystallographically independent molecules in the crystal lattice has enabled us to sample aspects of allowed conformational flexibility. The most dramatic feature of the structure, the large dihedral angle between the guanine bases, is similar in all four molecules of this X-ray structure and in the three solid-state structures of *cis*-[Pt(NH$_3$)$_2$[d(CpGpG)]]. This result implies that this aspect of the structure is imposed by chelation to platinum rather than by packing forces. Indeed, recent gel electrophoresis studies using site specifically platinated oligonucleotides have shown that the *cis*-[Pt(NH$_3$)$_2$[d(GpG)]] intrastrand crosslink results in a pronounced bend of the double helix toward the major groove at the site of platination.[64] Such bending would certainly be accompanied by a large dihedral angle between coordinated guanine rings, as found here.

Ultimately, we would like to apply knowledge of the X-ray structure of *cis*-[Pt(NH$_3$)$_2$[d(pGpG)]] to help understand the molecular mechanism by which *cis*-DDP exerts its antitumor activity. Since both *cis*-DDP and *trans*-DDP pass through cell membranes and bind to DNA, the different structures of their adducts with DNA are likely to be responsible for the widely different activities of the two isomers. The studies described here provide four detailed static pictures of the major adduct, an intrastrand d(GpG) crosslink, formed by *cis*-DDP with single-stranded DNA. From these pictures, some insight into the structures of adducts of *cis*-DDP with double-stranded DNA can be gained. Comparisons between backbone torsion angles from these studies and from theoretical models built by molecular mechanics calculations of platinum bound to both single- and double-stranded oligonucleotides[56] demonstrated many similarities.[17] The calculations suggest that the kind of structure described here might fit into double-helical DNA, either with local disruptions of Watson–Crick base pairing or duplex kinking, as found experimentally.[64] The orientation of guanine bases deduced from the double-stranded molecular mechanics models, however, differ

(60) Rosenberg, B.; Van Camp, L.; Trosko, J. E.; Mansour, V. H. *Nature (London)* **1969**, *222*, 385.
(61) Loehrer, P. J.; Einhorn, L. H. *Anna. Intern. Med.* **1984**, *100*, 704.
(62) (a) Blatter, E. E.; Vollano, J. F.; Krishnan, B. S.; Dabrowiak, J. C. *Biochemistry* **1984**, *23*, 4817. (b) Rotondo, E.; Fimiani, V.; Cavallaro, A.; Ainis, T. *Tumori* **1983**, *69*, 31. (c) Elespuru, R. K.; Daley, S. K. In *Platinum Coordination Complexes in Cancer Chemotherapy*; Hacker, M. P., Douple, E. B., Krakoff, I. E., Eds.; Martinus Nijhoff Publishers: Boston, 1984; p 58. (d) Vrâna, O.; Brabec, V.; Kleinwächter, V. *Anti-Cancer Drug Design* **1986**, *1*, 95.
(63) Schöllhorn, H.; Beyerle-Pfnür, R.; Thewalt, U.; Lippert, B. *J. Am. Chem. Soc.* **1986**, *108*, 3680.
(64) Rice, J. A.; Pinto, A. L.; Lippard, S. J.; Crothers, D. M. *Proc. Natl. Acad. Sci. U.S.A.* **1988**, *85*, 4158.

somewhat from those in *cis*-[Pt(NH$_3$)$_2$\{d(pGpG)\}]. Base/base dihedral angles in the theoretical models range from 50°–66°, a significant reduction from the angles observed here. Moreover, diminished N7–Pt–N7 angles of 79°–82° occur in the models from molecular mechanics calculations, which partly accounts for the smaller base/base dihedral angles. Comparatively reduced base/PtN$_4$ angles, ranging from 52°–85°, are also observed in the theoretical double-stranded models. Comparisons between B-DNA and *cis*-[Pt(NH$_3$)$_2$\{d(pGpG)\}] in Figure 11 suggest that the structures revealed by the present X-ray study could not exist in double-stranded DNA without either significant disruption of hydrogen bonds involved in Watson–Crick base pairing or considerable distortion of the complementary strand. The gel electrophoresis data suggest DNA bending of ~40°±5° accompanies formation of the d(GpG) *cis*-diammineplatinum(II) crosslink. Such a distortion in the duplex would undoubtedly influence cellular phenomena such as DNA repair.

The crystallization and X-ray structural elucidation of platinum complexes of double-stranded oligonucleotides would provide much needed structural information about both the site of platination and duplex perturbations several base pairs away from the site of platination. Such information would be very helpful in interpreting the results of the biochemical processing of DNA, both in vitro and in vivo.[65] Crystallization of *cis*-diammineplatinum(II) adducts with single-stranded oligonucleotides containing extra bases at the 5′- or 3′-ends of d(pGpG) will probably not supply much additional information to that which we already have. As in the case of the 5′-cytosine in the X-ray structure of *cis*-[Pt(NH$_3$)$_2$\{d(CpGpG)\}], the conformations of 5′- or 3′-bases in single-stranded oligonucleotides will be highly influenced by crystal packing forces in the solid state. X-ray studies of other adducts formed by *cis*-DDP and adducts formed by *trans*-DDP, however, will provide needed structural information.

Acknowledgment. This work was supported by U.S. Public Health Service Grant CA 34992 (to S.J.L.) from the National Cancer Institute. D.G. was a Chain Weizmann Postdoctoral Fellow. Helpful discussions, advice, and experimental assistance were provided by Professor G. Petsko, Drs. G. J. Quigley, J. Kozelka, P. Shing Ho, C. Frederick, P. Mascharak, and R. Campbell, to whom we are grateful. We also thank the Engelhard Corporation for a loan of K_2PtCl_4 from which the platinum dinucleotide complex was prepared.

Registry No. *cis*-[Pt(NH$_3$)$_2$(d(pGpG))], 81119-95-1.

Supplementary Material Available: Tables of atomic positional and thermal parameters (Tables S2 and S3), interatomic bond distances and angles (Tables S4 and S5), and best planes calculations (Table S6) (17 pages); observed and calculated structure factor amplitudes (Table S1) (61 pages). Ordering information is given on any current masthead page.

(65) For recent results on site specifically platinated DNAs containing the *cis*-[Pt(NH$_3$)$_2$\{d(GpG)\}] adduct, see: (a) Pinto, A. L.; Naser, L. J.; Essigmann, J. M.; Lippard, S. J. *J. Am. Chem. Soc.* **1986**, *108*, 7405. (b) Naser, L. J.; Pinto, A. L.; Lippard, S. J.; Essigmann, J. M. *Biochemistry* **1988**, *27*, 4357.

Ruthenium(II) 2,2′-Bipyridine Complexes Containing Methyl Isocyanide Ligands. Extreme Effects of Nonchromophoric Ligands on Excited-State Properties

Maria Teresa Indelli, Carlo Alberto Bignozzi, Anna Marconi, and Franco Scandola*

Contribution from the Dipartimento di Chimica dell'Università, Centro di Fotochimica C.N.R., I-44100 Ferrara, Italy. *Received January 7, 1988*

Abstract: The new isocyanide complexes Ru(bpy)$_2$(CN)(CNMe)$^+$, Ru(bpy)$_2$(CNMe)$_2^{2+}$, and Ru(bpy)(CNMe)$_4^{2+}$ have been synthesized, and their photophysical and redox behavior has been studied in detail. With respect to the cyanide analogues, the strong electron-withdrawing effect of the methyl isocyanide ligands causes (i) large blue shifts in the Ru→bpy MLCT transitions and (ii) large anodic shifts in the potentials for oxidation of Ru(II). The excited-state behavior of Ru(bpy)(CNMe)$_4^{2+}$ appears quite exceptional with respect to that of common Ru(II) bipyridine complexes. In fact (i) its lowest excited state is a long lived (τ = 8.8 μs in water at 298 K) bpy-centered π–π^* state and (ii) the complex is a strong excited-state oxidant ($E_{1/2}$(*Ru(III)/Ru(II)) = +1.49 V vs SCE in MeCN). This constitutes a rather extreme example of tuning of excited-state properties by nonchromophoric ligands.

Because of its outstanding excited-state properties, tris(2,2′-bipyridine)ruthenium(II), Ru(bpy)$_3^{2+}$, has been one of the most extensively studied and widely used molecules in research laboratories during the last 10 years.[1-3] It is now clear that, at least in room temperature fluid solution, the d–π^* metal-to-ligand charge transfer (MLCT) excited state of Ru(bpy)$_3^{2+}$ is localized on a single Ru–bpy unit.[4] Common mono- or bis-2,2′-bipyridine (2,2′-bipyridine = bpy) ruthenium(II) complexes containing non-polypyridine ancillary ligands, however, do not exhibit the outstanding excited-state properties of the parent Ru(bpy)$_3^{2+}$ complex.[2,3] This is generally due to fast deactivation of the relevant Ru–bpy d–π^* (MLCT) excited state occurring via low-lying d–d metal centered (MC) states.[5-7] The only way to avoid this process and to obtain mono- and bis-bpy Ru(II) complexes of appreciable excited-state lifetime is to use very strong field nonchromophoric ligands. Thus, mixed cyanide–bpy complexes such as Ru(bpy)$_2$(CN)$_2$[8] and, more recently, Ru(bpy)(CN)$_4^{2-}$[9] have been

(1) Kalyanasundaram, K. *Coord. Chem. Rev.* **1982**, *46*, 159.
(2) Seddon, E. A.; Seddon, K. *The Chemistry of Ruthenium*; Elsevier: Amsterdam, 1984; Chapter 15.
(3) Juris, A.; Barigelletti, F.; Campagna, S.; Balzani, V.; Belser, P.; von Zelewsky, A. *Coord. Chem. Rev.* **1988**, *84*, 85.
(4) Evidence for this conclusion comes from a wide variety of experimental techniques. For a discussion on this point, see section 4-C of ref 3, and references therein.
(5) Caspar, J. V.; Meyer, T. J. *Inorg. Chem.* **1983**, *22*, 2444.
(6) Meyer, T. J. *Pure Appl. Chem.* **1986**, *58*, 1193.
(7) Wacholtz, W. M.; Auerbach, R. A.; Schmehl, R. H.; Ollino, M.; Cherry, W. R. *Inorg. Chem.* **1985**, *24*, 1417.
(8) Demas, J. N.; Addington, J. W.; Peterson, S. H.; Harris, E. W. *J. Phys. Chem.* **1977**, *81*, 1039.

0002-7863/88/1510-7381$01.50/0